Journal of Physical and Chemical Reference Data

RESEARCH ARTICLE | JUNE 28 2023

Cross Sections for Electron Collisions with N_2, N_2^*, and N_2^+

Mi-Young Song ; Hyuck Cho; Grzegorz P. Karwasz ; Viatcheslav Kokoouline ; Jonathan Tennyson

Journal of Physical and Chemical Reference Data 52, 023104 (2023)
https://doi.org/10.1063/5.0150618

Journal of Physical and Chemical Reference Data ARTICLE scitation.org/journal/jpr

Cross Sections for Electron Collisions with N_2, N_2^*, and N_2^+

Cite as: J. Phys. Chem. Ref. Data 52, 023104 (2023); doi: 10.1063/5.0150618
Submitted: 15 March 2023 • Accepted: 27 April 2023 •
Published Online: 28 June 2023

Mi-Young Song,[1,a)] Hyuck Cho,[2] Grzegorz P. Karwasz,[3] Viatcheslav Kokoouline,[4] and Jonathan Tennyson[5]

AFFILIATIONS

[1] Institute of Plasma Technology, Korea Institute of Fusion Energy (KFE), 37 Dongjangsan-ro, Gunsan, Jeollabuk-do 54004, South Korea
[2] Department of Physics, Chungnam National University, Daejeon 34134, South Korea
[3] Institute of Physics, Astronomy and Applied Informatics, Nicolaus Copernicus University, Grudziadzka 5, 87-100 Toruń, Poland
[4] Department of Physics, University of Central Florida, Orlando, Florida 32816, USA
[5] Department of Physics and Astronomy, University College London, Gower Street, London WC1E 6BT, United Kingdom

[a)] **Author to whom correspondence should be addressed:** mysong@kfe.re.kr

ABSTRACT

Electron collision cross section data are complied from the literature for electron collisions with the nitrogen molecules, N_2, N_2^+, and N_2^*. Cross sections are collected and reviewed for total scattering, elastic scattering, momentum transfer, rotational excitation, vibrational excitation, electronic excitation, dissociative processes, and ionization. The literature has been surveyed up to the end of 2021. For each of these processes, the recommended values of the cross sections are presented.

Published by AIP Publishing on behalf of the National Institute of Standards and Technology. https://doi.org/10.1063/5.0150618

Key words: attachment; dissociation; electron collisions; evaluation; ionization; total cross sections.

CONTENTS

List of Tables

List of Figures

1. Introduction

Molecular nitrogen, N_2, is the major component of the Earth's atmosphere, which means that electron collisions with nitrogen occur both naturally, for example, in lightning strikes, and in many applications. This has led to nitrogen plasmas being an important topic of study in plasma physics; as N_2 is strongly bound, these plasmas occur for a wide range of temperatures. Besides the Earth's atmosphere, N_2 is present in many other atmospheres in the solar system, notably Titan, where it comprises 98.4% of the atmosphere, Venus (3.5%) and Mars (1.9%),[1] as well as Triton[2] and Pluto.[3] It is thought to be a major atmospheric component in rocky exoplanets (e.g., the work of Rimmer and Rugheimer[4] and Tsiaras *et al.*[5]). Electric fields cause giant electric discharges at the top of planetary atmospheres, including our own, called sprites, which can be observed[6] through spontaneous emission from excited electronic states of N_2; similar N_2 afterglows can be observed in laboratory plasmas.[7,8]

Models of spacecraft re-entry and studies of hypersonic flows,[9,10] as well as other shock waves,[11] rely on a detailed understanding of the interactions of electrons with N_2 and N_2^+ as well as metastable excited states, which are generally denoted N_2^*. Indeed, a feature of nitrogen plasmas is the characteristic emissions from various (metastable) electronically excited states of the molecule.[12–14] In the industrial process field, nitrogen plasma transmits and diffuses nitrogen ions in plasma to metal/non-metal surfaces and is used as a surface hardening method of materials.[15]

There are numerous examples of technological and other uses of nitrogen plasma chemistry. For example, N_2 can be used as a seeding gas in magnetically confined fusion plasmas (ITER and JET experiments) to help in the reduction of power loads on the divertor region.[16] Nitrogen plasmas can be used to initiate chemical processes.[8,17] Of course, all atmospheric plasmas necessarily involve N_2.

Due to the importance of low-temperature nitrogen plasmas, there have been many attempts to build nitrogen plasma kinetic models (or plasma chemistries),[11,18–25] which involve processes initiated by both electron and heavy particle collisions. The current evaluation of available data on electron collision processes with N_2, N_2^+, and N_2^* will provide important input into these models.

The present paper is based both on experimental and on recent theoretical results. To some extent, it is complementary and/or supersedes earlier, similar compilations. Itikawa[26] gave an excellent review, based mainly on experiments, of total and partial cross sections for the N_2 molecule: Our work includes also cross sections for metastable N_2^* states and the N_2^+ ion. Tabata *et al.*[27] gave analytic approximations over in a broad energy range for 74 processes involving electron collisions N_2 and N_2^+, which also include cross sections for the optical emission. However, since these studies, new data (measurements and calculations) on the rotational, vibrational, and electronic excitations have appeared that differ significantly from earlier values. More recently, Kawaguchi, Takahashi, and Satoh[28] not only gave recommended cross sections (for the N_2 molecule) but also calculated transport coefficients (drift velocities, longitudinal, and transversal diffusion, etc). We find their much of their data congruent with the present analysis. Furthermore, for plasma modeling, particularly in nitrogen, knowledge of cross sections involving metastable and ionized species is needed.

2. N_2 Molecule

2.1. Total scattering cross section

Measurements of total cross sections (TCSs) in N_2 served for more than 40 years as a check of performance of experimental setups. The discovery of the vibrational structure in the resonant maximum of the TCS by Schulz[29] was one of the milestones in atomic and molecular physics. Precise measurement of this structure with a time-of-flight apparatus (i.e., with an intrinsic determination of the collision energy) by Kennerly[30] established a reference for the energy scale calibration for all consecutive studies, in which bias contact potentials influenced this calibration in an unknown manner (see, for example, the work of Karwasz, Brusa, and Pliszka).[31] In our previous paper[32] on CH_4, we discussed some more aspects of methodologies in TCS experiments. Furthermore, we refer the reader to other reviews[33–35] on experimental techniques, which gave TCS also for N_2.

Agreement between different experiments (see Fig. 1) is to be considered excellent; existing discrepancies are well explained by particular features of the equipment used: The electron/positron experiment by Hoffman *et al.*[36] was not designed for very high energy resolution; the difficulties in precise timing and beam focusing led to the measurements of Kennerly,[30] giving underestimates at 50 eV. A similarly difficulty was the timing in the electron and positron experiment of Sueoka and Mori,[37] so they used an "effective" length of the scattering cell, therefore introducing some systematic uncertainty.

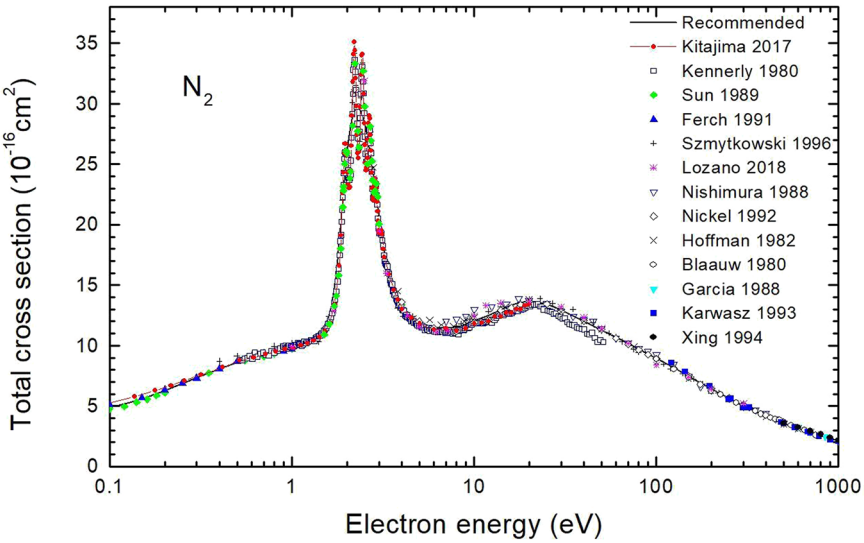

FIG. 1. Experimental TCS for N_2. Data, in order of increasing energy, are from the work of Kitajima *et al.*[38]—red circles; Kennerly[30]—blue open squares; Sun *et al.*[39]—green diamonds; Ferch, Raith, and Schweiker[40]—blue up triangles; Szmytkowski, Maciag, and Karwasz[33]—black crosses; and Lozano *et al.*[41]—magenta asterisks.

From Fig. 1, we excluded the very low energy measurements by Jost *et al.*[42] obtained with an electrostatic-beam apparatus (published only as a curve in conference abstracts) and those of Hoffman *et al.*[43] who made an avant-garde use of synchrotron radiation as the source of near-to-zero energy electrons. However, Hoffman and Lunt[43] were only able to measure the gross part of the forward and backward scattered electrons, so their data do not constitute the cross sections *in sensu stricte*. A further development of that technique at the Tsukuba KEK synchrotron source[44] allows measurements down to 5 meV and with a constant energy resolution, up to 20 eV collision energy (see Fig. 2).

Conversely, the energy resolution changes with the collision energy in the time-of-time technique.[30,37,39,40] In the experiment of Sun *et al.*,[39] the energy resolution varied from 10 meV at the very low-energy limit to around 50 meV at 2.5 eV; the uncertainty in the energy scale bias varied from 1 meV at 0.01 eV to about 50 meV at 2.5 eV. On the other hand, the energy resolution of the electrostatic spectrometer from the Gdańsk Technical University[33] was constant over the whole low-energy range—somewhat better than 70 meV. Kitajima *et al.*,[38] in contrast to several earlier experiments, in particular, from those with electrostatic spectrometers[33,46] and magnetically focused beams,[36,37,41] did not use the resonant structure at about 2.4 eV as measured by Kennerly[30] but calibrated their absolute energy scale against a narrow (1.5 meV) Feshbach resonance N_2^- ($R\ ^2\Sigma_g^+$) with a well-pronounced Fano profile, at 14.5 eV (see the graphical abstract linked to the paper of Kitajima *et al.*[38]). The position of this resonance was established as 11.497(2) eV in a joint theoretical-experimental study,[47] which used simultaneous measurements with the Ar^- ($^2P_{3/2}$) Feshbach resonance located at 11.103(1) eV.

A comparison of the $^2\Pi_g$ resonant structure in the TCS at about 2.4 eV as seen in different experiments[30,33,38,39] is given in Fig. 2. On average, the difference in resonance peaks positions between the TCS of Kitajima *et al.*[38] and those by Kennerly[30] is −10 meV. This is slightly outside the uncertainty for these positions given by Kitajima *et al.*[38] Therefore, at present, we recommend the vibrational $^2\Pi_g$ structure of Kitajima *et al.*[38] as the reference measurement. This choice needs an additional experimental (and theoretical) check, as it could influence the energy scaling of many previous experiments on numerous atomic and molecular targets. In the very low energy range, i.e., below 1 eV measurements by different methods[30,33,38–40] agree within their error bars (see Fig. 3), and also with present integral (vibrationally) elastic cross sections, and pretty well with the recommended vibrationally elastic integral cross sections (ICSs) of Kawaguchi, Takahashi, and Satoh.[28] Modified-effective range theory (MERT)[48] allows extension of the TCSs (which equals the integral elastic cross section in the very-low range) to $E = 0$ (see Fig. 3): The zero-energy cross sections from MERT applied to TCS[48] and from the swarm analysis of Kawaguchi, Takahashi, and Satoh[28] equal to 1.1 and 1.01 Å^2, respectively.

At the high energy limit (above 1000 eV), the measurements by Karwasz *et al.*[49] are systematically underestimated due to the lack of the energy retarding-field analyzer; the experiment by García, Pérez, and Campos[50] was free from this drawback. The Born–Bethe fit,

$$\sigma(E) = \frac{A}{E} + B\frac{\log E}{E}, \tag{1}$$

where the energy is expressed in Rydbergs, $R = 13.6$ eV, and the cross sections is expressed in atomic units $a_0^2 = 0.28 \times 10^{-16}$ cm^2, allows identification of possible systematic errors in the high energy limit and extrapolation of the TCS up to a few tens of keV (see Fig. 4). As seen from this figure, the TCS in the high energy range can be well fitted by a straight-line with $A = -60$ and $B = 310$ [in the units of Eq. (1)]. Recommended cross sections from 0.1 to 1000 eV are

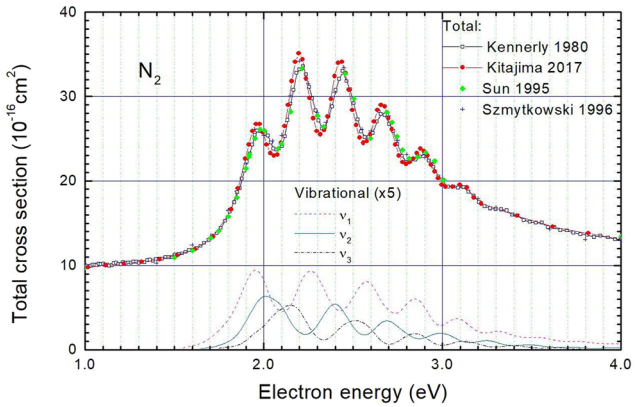

FIG. 2. TCS in the region of the $^2\Pi g$ resonance: Comparison of two benchmark measurements by Kennerly[30] time-of-flight (blue open squares) and the synchrotron-based electron source by Kitajima *et al.*[38] Additionally, the time-of-flight results by Sun *et al.*[39] (green diamonds) are shown and from the electrostatic beam by Szmytkowski, Maciag, and Karwasz[33] (crosses). Integral vibrational (multiplied by 5) are from the work of Allan.[45] We recommend the more recent result by Kitajima *et al.*[38]

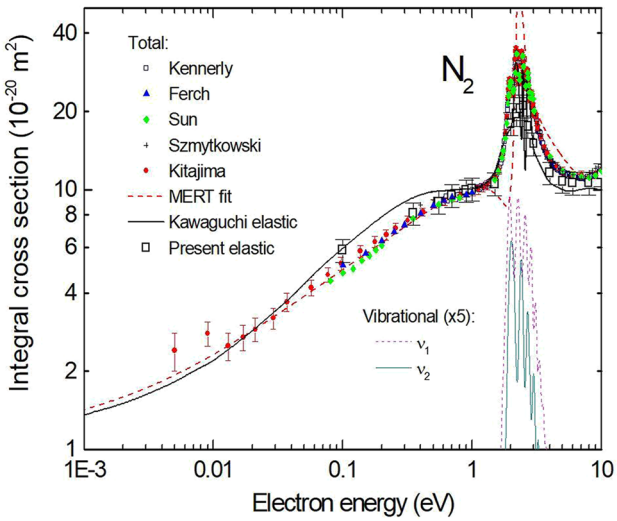

FIG. 3. TCS in the very-low energy limit. Symbols are the same as in Fig. 1, apart from black open big squares with error bars that present recommended integral elastic cross sections; the black thick line is the integral elastic used by Kawaguchi, Takahashi, and Satoh;[28] MERT-fit is the analysis by Idziaszek and Karwasz,[48] *d*-wave resonance and vibrational data (multiplied by 5) are by Allan.[45]

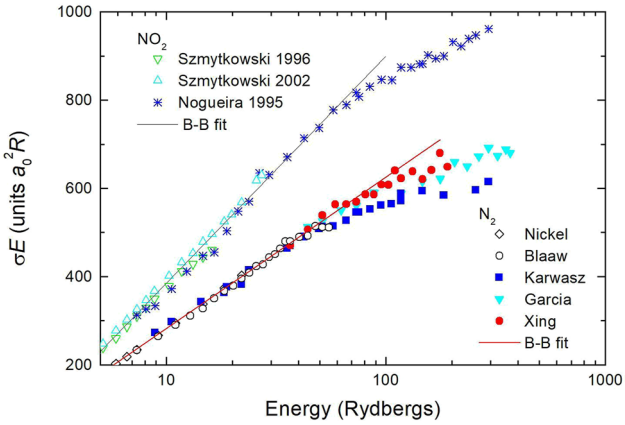

FIG. 4. High-energy extrapolation of TCS via Bethe–Born fit of Eq. (1). We compare here N_2 with NO_2 that was the subject of our previous review.[51] The comparison shows that in the high energy range, TCS tends to be underestimated: This is the case of measurements from Trento laboratory by Zecca *et al.*[52] in NO_2 and by Karwasz *et al.*[49] in N_2.

given in Table 1. The uncertainty of the recommended data is 5%, except for energies below 1 eV and above 700 eV where it is 10%. Detailed cross sections in the region of the $^2\Pi_g$ resonance are given in Table 2.

2.2. Elastic scattering cross section

Vibrationally elastic cross sections for the nitrogen molecule have been measured and reported by many laboratories. In this evaluation, we used the data from the following reports: Srivastava, Chutjian, and Trajmar,[53] Shyn and Carignan,[54] Sohn *et al.*,[55] Nickel *et al.*,[56] Brennan *et al.*,[57] Shi, Stephen, and Burrow,[58] Sun *et al.*,[39] Zubek, Mielewska, and King,[59] Allan,[60] Muse *et al.*,[61] and Linert and Zubek.[62] In most of these experiments, a crossed-beam apparatus employing an electrostatic monochromator and an analyzer was used. Their angular ranges vary mostly from around 10°–140°, except by Zubek, Mielewska, and King,[59] Allan,[60] and Linert and Zubek,[62] in which angle-changing devices were used to cover up to 180°. Among these reports, we chose one specific dataset at one electron energy or average more than one datasets to derive recommended elastic differential cross sections (DCSs). While most measurements have been performed down to around 0.5 eV incident electron energy, Sohn *et al.*[55] measured down to the energy of 0.1 eV, which is uniformly lower than the others.[39,59,61] When we renormalized Sohn's data by a factor of 1.4, it agreed quite well with others at 0.55 and 1.0 eV. Therefore, our recommended elastic DCS at 0.1 eV was obtained by multiplying Sohn's data by a factor of 1.4. The recommended elastic DCSs are shown in Fig. 5 and Table 3, respectively. For elastic ICS, there is a relatively recent recommendation by Itikawa.[26] Itikawa derived his recommended elastic ICS by combining the previous recommendation by Buckman, Brunger, and Elford[63] at 0.55–100 eV with two sets of beam experiments by Shyn and Carignan[54] and DuBois and Rudd[64] at 100 eV to extend the recommended data up to 1000 eV. The elastic ICSs between 1 and 4 eV in Fig. 6 and Table 4 show only an envelope of the resonance. Buckman *et al.*'s evaluation was based on the results of the beam experiments.[39,53–55,57,58] Basically, we adopted the evaluation by Itikawa[26] but again extended to the electron energy of 0.1 eV in the same way as we did for the elastic DCS. In other words, at 0.1 eV, we renormalized the elastic ICS of by Sohn *et al.*[55] by a factor of 1.4. In addition, at 0.55 and 1.0 eV, slight modifications were made to Itikawa's ICS, by including the renormalized ICS of Sohn *et al.* at those energies. From 1.5 to 1000 eV, Itikawa's ICSs are adopted unchanged. The uncertainties vary from 6% to 15% for DCS and about 10%–20% for ICS.

TABLE 1. Recommended TCS for electron scattering on N_2. Data are based on those by from the review by Karwasz *et al.*[34] In the resonance region (2.5–3.5 eV), data in this table are averaged over the vibrational structure. For details, see Table 2

Energy (eV)	TCS (10^{-16} cm^2)	Energy (eV)	TCS (10^{-16} cm^2)
0.1	4.88	12.0	12.4
0.12	5.13	15.0	13.2
0.15	5.56	17.0	13.5
0.17	5.85	20.0	13.7
0.2	6.25	25.0	13.5
0.25	6.84	30.0	13.0
0.3	7.32	35.0	12.4
0.35	7.72	40.0	12.0
0.4	8.06	45.0	11.6
0.45	8.33	50.0	11.3
0.5	8.61	60.0	10.7
0.6	8.96	70.0	10.2
0.7	9.25	80.0	9.72
0.8	9.48	90.0	9.30
0.9	9.66	100	8.94
1.0	9.85	120	8.33
1.2	10.2	150	7.48
1.5	11.2	170	7.02
1.7	13.3	200	6.43
2.0	25.7	250	5.66
2.5	28.5	300	5.04
3.0	21.0	350	4.54
3.5	14.6	400	4.15
4.0	13.2	450	3.82
4.5	12.3	500	3.55
5.0	11.8	600	3.14
6.0	11.4	700	2.79
7.0	11.4	800	2.55
8.0	11.5	900	2.32
9.0	11.7	1000	2.13
10.0	12.0		

2.3. Momentum transfer cross section

Momentum transfer cross sections (MTCSs) are measured by one of two methods: electron–molecule crossed beam or swarm experiments. In most crossed beam experiments mentioned in Sec. 2.2 on elastic cross sections,[53–62] the elastic MTCSs for electron scattering on nitrogen molecules are presented or, at least, can be derived from their elastic DCSs. However, the limitations of the crossed beam methods means that the incident electron energies

TABLE 2. Recommended TCS for electron scattering on N_2 in the region of the $^2\Pi$ shape resonance. Data are those by Kitajima *et al.*[38]

Energy (eV)	TCS (10^{-16} cm^2)	Energy (eV)	TCS (10^{-16} cm^2)
3.417	15.9	2.457	32.8
3.217	17.3	2.437	34.1
3.177	18.0	2.417	34.0
3.137	19.2	2.397	32.4
3.097	19.5	2.377	29.7
3.057	19.3	2.357	27.6
3.017	19.3	2.337	26.0
2.997	19.5	2.317	25.5
2.977	20.3	2.297	25.9
2.957	21.1	2.277	27.4
2.937	21.9	2.257	29.8
2.917	23.0	2.237	32.1
2.897	23.5	2.217	34.4
2.877	23.8	2.197	35.1
2.857	23.3	2.177	34.1
2.837	22.6	2.157	31.8
2.817	22.2	2.137	29.0
2.797	22.0	2.117	26.5
2.777	22.2	2.097	24.5
2.757	23.0	2.077	23.1
2.737	24.3	2.057	23.0
2.717	26.1	2.037	23.3
2.697	27.4	2.017	24.3
2.677	28.8	1.997	25.7
2.657	29.0	1.977	26.7
2.637	28.4	1.957	26.7
2.617	27.0	1.937	25.9
2.597	25.5	1.917	24.3
2.577	24.7	1.897	22.6
2.557	24.5	1.857	19.1
2.537	25.1	1.817	16.6
2.517	26.6	1.717	13.4
2.497	28.4	1.617	11.9
2.477	30.8	1.517	11.2

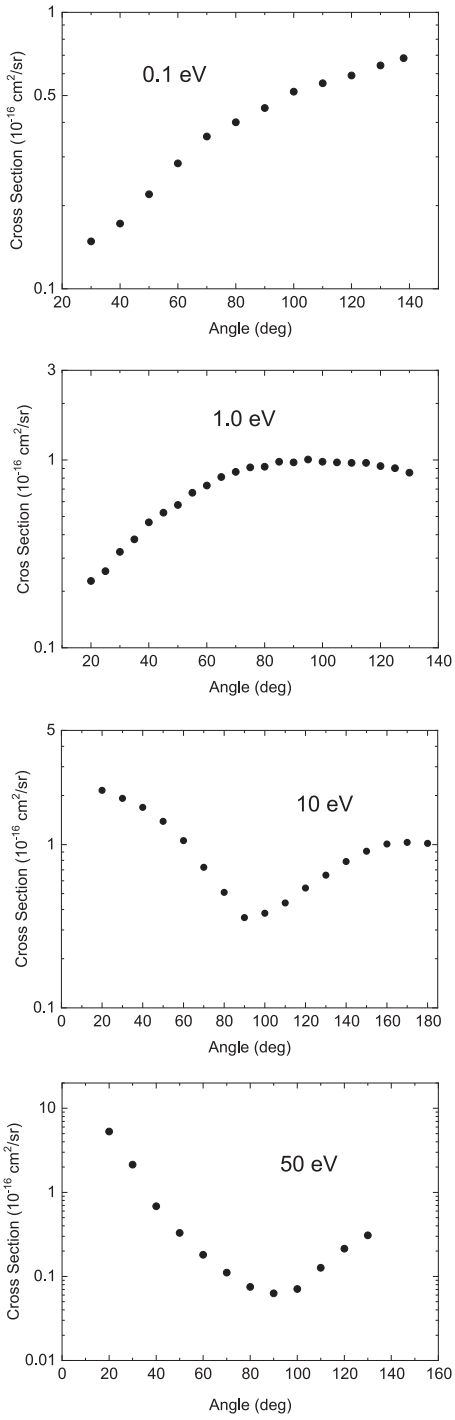

FIG. 5. Recommended elastic DCS of N_2 (10^{-16} cm^2/sr).

are typically higher than 0.1 eV. The lower electron energy region can be covered by swarm methods. The recommended MTCSs can be derived from one of these two methods or, more generally, from a combination of both, sometimes together with theoretical calculations. Previously, Elford, Buckman, and Brunger[65] and Itikawa[26] compiled the MTCSs from the various reports and gave the recommended MTCSs. Itikawa,[26] based also on the study by Elford, Buckman, and Brunger,[65] derived the recommended MTCS from the swarm experiment by Haddad[66] for 0.001–0.5 eV, an experiment by Sun *et al.*[59] in the resonance region 0.5–3.5 eV, and experiments by Sun *et al.* and Srivastava *et al.*[53] above 4 eV. Very recently, Kawaguchi *et al.*[28] recommended MTCSs with a set of cross sections for other processes after assessing extensive cross section databases in the electron energy range from 10^{-3} to 10^4 eV. Their recommended MTCSs overlap well with the beam measurements[53–55,58,61,62,64] from 0.1 to 400 eV and also with the recommendation by Itikawa[26] with a slight deviation in the intermediate energy region. Kawaguchi presented no uncertainties. Since Kawaguchi's recommended data were derived from extensive theoretical and experimental reports on the MTCSs of N_2, many of which

TABLE 3. Recommended elastic DCS of N_2 (10^{-16} cm^2 sr^{-1})

Angle (deg)	0.1 eV DCS	0.55 eV DCS	1.0 eV DCS	3.0 eV DCS	5.0 eV DCS	10.0 eV DCS	20.0 eV DCS	50.0 eV DCS	100.0 eV DCS	200 eV DCS	300 eV DCS	400 eV DCS
10					1.291		6.824		11.485	8.240	5.867	5.493
20			0.227	2.757	1.393	2.147	4.137	5.301	3.326	1.85	1.094	0.845
30	0.1484	0.306	0.324	2.384	1.489	1.918	2.472	2.134	0.906	0.455	0.32	0.311
40	0.1722	0.385	0.466	1.929	1.457	1.688	1.642	0.684	0.361	0.204	0.17	0.161
50	0.2198	0.461	0.576	1.466	1.355	1.386	1.036	0.33	0.172	0.137	0.099	0.078
60	0.2842	0.58	0.731	1.081	1.176	1.058	0.633	0.181	0.109	0.096	0.058	0.047
70	0.3556	0.685	0.864	0.814	0.933	0.726	0.347	0.111	0.078	0.065	0.04	0.037
80	0.4004	0.761	0.921	0.686	0.741	0.510	0.204	0.075	0.072	0.048	0.035	0.028
90	0.4508	0.819	0.970	0.626	0.645	0.357	0.205	0.063	0.074	0.042	0.032	0.022
100	0.5166	0.868	0.978	0.631	0.581	0.380	0.261	0.071	0.075	0.041	0.028	0.019
110	0.5544	0.888	0.965	0.694	0.575	0.439	0.356	0.127	0.085	0.044	0.023	0.017
120	0.5908	0.896	0.928	0.791	0.601	0.542	0.473	0.214	0.105	0.048	0.023	0.016
130	0.6426	0.924	0.856	1.069	0.626	0.65	0.577	0.308	0.13	0.052	0.024	0.016
140					0.684	0.788	0.715					
150					0.754	0.91	0.914					
160					0.85	1.008	1.064					
170					0.92	1.031	1.147					
180					0.933	1.016	1.223					

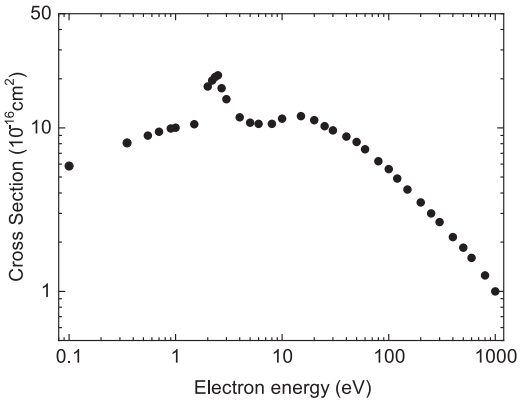

FIG. 6. Recommended elastic ICS of N_2.

TABLE 4. Recommended elastic ICS of N_2 in the units of 10^{-16} cm^2. Energy in eV

Electron energy (eV)	ICS (10^{-16} cm^2)	Electron energy (eV)	ICS (10^{-16} cm^2)
0.1	5.84	20	11.15
0.35	8.09	25	10.25
0.55	8.96	30	9.65
0.7	9.48	40	8.85
0.9	9.91	50	8.2
1.0	10.03	60	7.4
1.5	10.53	80	6.25
2.0	17.93	100	5.6
2.2	19.5	120	4.9
2.35	20.5	150	4.2
2.5	21.0	200	3.5
2.7	17.5	250	3.0
3.0	15.0	300	2.65
4.0	11.6	400	2.15
5.0	10.75	500	1.85
6.0	10.6	600	1.60
8.0	10.6	800	1.25
10	11.4	1000	1.00
15	11.8		

do not provide any information on the uncertainties, it is difficult to estimate uncertainties to a reasonable figure. However, the most experimental MTCSs have uncertainties of not more than a few percent, and similarly good calculations of the MTCSs usually agree with existing measured MTCSs within a few percent. Therefore, it could be concluded that for the majority of energies of the cross sections, the uncertainties would be of the order of a few percent. Here, we recommend the results by Kawaguchi for MTCS, presented in Fig. 7 and Table 5. A more complete dataset can be obtained directly from Ref. 28.

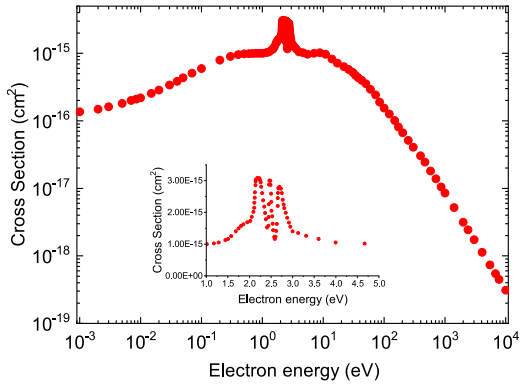

FIG. 7. Recommended elastic MTCS of N_2.

TABLE 5. Recommended elastic MTCS of N_2 in the units of 10^{-16} cm^2. Energy in eV

Electron energy (eV)	MTCS (10^{-16} cm^2)	Electron energy (eV)	MTCS (10^{-16} cm^2)
0.001	1.36	30.7	5.21
0.02	2.85	50.4	3.55
0.03	3.4	72.5	2.42
0.04	3.85	84.7	1.89
0.05	4.33	100	1.54
0.1	5.95	150	1.01
0.2	7.9	202	0.665
0.3	9.0	303	0.407
0.4	9.59	398	0.305
0.5	9.8	471	0.245
0.6	9.87	579	0.181
0.7	9.95	713	0.139
0.8	10.0	867	0.105
0.9	10.0	1 000	0.085
1.0	10.0	1 995	0.032
2.02	17.3	3 020	0.017
3.0	14.0	4 074	0.011
4.0	10.5	5 495	0.007
10.9	9.72	7 762	0.004
21.9	6.33	10 000	0.003

2.4. Rotational excitation cross sections

The main nitrogen isotope ^{14}N has a nuclear spin 1, so its nucleus is a boson. Therefore, the total wave function of the $^{14}N_2$ molecule does not change under a permutation (12) of the two identical nuclei in $^{14}N_2$. The permutation affects the nuclear and electronic spins as well as electronic and rotational coordinates of the molecule. The allowed values of the total nuclear spin I of the $^{14}N_2$ molecule are 0, 1, and 2. The nuclear spin function is invariant under (12) for $I = 0$ and 2 and changes sign for $I = 1$. The ground electronic state $X\ ^1\Sigma_g^+$ of N_2 is invariant under (12). Rotational wave functions are invariant for the even rotational angular momentum j and change sign under (12) for odd j. Therefore, for $I = 0, 2$ nuclear spin (ortho-$^{14}N_2$), only even j are allowed, and for $I = 1$ nuclear spin (para-$^{14}N_2$), only odd j are allowed.

The nucleus of the second most abundant isotope ^{15}N is a fermion with the nuclear spin 1/2 so that the total wave function of the $^{15}N_2$ molecule changes sign under (12). It implies that for the ortho-$^{15}N_2$ molecule with $I = 1$, only odd j are allowed, while for para-$^{15}N_2$, even-j are allowed in the ground electronic state.

In collisions with an electron, if the electronic state of N_2 is unchanged, for example, the molecule is in the ground electronic state before and after the collision, electron-impact induced transitions are allowed only between rotational states of the same parity, i.e., only the $\Delta j = 2, 4, \ldots$ transitions are allowed. This is due to the combined effect of the requirements: (a) The parity (gerade/ungerade) of the total electronic wave function of the $N_2 + e^-$ system is conserved during the collision because the molecule is diatomic and homonuclear and (b) the total parity of the system, including the rotational wave function, is also conserved.[67]

Data on rotational excitation available before 2006 were reviewed by Itikawa and Mason[68] and by Itikawa.[26]

Cross sections for rotational excitation for transitions between the lowest even j have been computed in several previous studies. Kutz and Meyer[69] calculated cross sections for transitions $j = 0 \rightarrow 2, 4, 6$ using the closed-coupling method with a local correlation-polarization-exchange potential to evaluate the scattering at a fixed geometry and the adiabatic nuclei approximation (the rotational frame transformation). Morisson *et al.*[70] determined the $j = 0 \rightarrow 2$ cross sections using the body-frame electron–molecule scattering matrix obtained using MERT and then analytically corrected to obey threshold laws. Telega, Bodo, and Gianturco[71] computed the $j = 0 \rightarrow 2, 4$ cross sections using a multichannel close-coupling approach, treating the rotational motion of N_2 explicitly in the closed-coupled equations. The $N_2 + e^-$ potential in the study accounts for static, exchange, and correlation-polarization contributions. In 2011, Šulc *et al.*[72] reported the theoretical cross section for the $j = 0 \rightarrow 2$ transition, evaluating the scattering at a fixed geometry and applying the adiabatic nuclei approximation similarly to Kutz and Meyer.[69] The fixed-nuclei scattering was obtained in a body-fixed reference frame with the same potential interaction as the one used by Telega, Bodo, and Gianturco.[71] We also note the $j = 0 \rightarrow 2$ theoretical cross section available in the IST-Lisbon database,[73] which appear to be derived from a relatively old estimate. All these data are shown in Fig. 8.

In preparing this paper, we also computed the $j = 0 \rightarrow 2, 4$ cross section over a wide interval of energies, up to 10 eV. The calculations were performed using the UK molecular R-matrix code[74] as implemented in QEC[75] with a static-exchange plus polarization (SEP) model using a `cc-pVTZ` basis set. The present results are also shown in Fig. 8. As one can see, the present calculations agree well with the most recent theoretical study by Šulc *et al.*[72] in the energy interval covered by Šulc *et al.*[72] We recommend using the cross section computed in the present study, which are given in Table 6.

No cross sections for transitions between odd j (para-$^{14}N_2$ and ortho-$^{15}N_2$) are available in the literature. For the mixed isotopologues, such as $^{14}N^{15}N$, odd and even j are allowed for any total nuclear spin. In addition, in the isotopologues, $\Delta j = 1$ transitions are allowed and driven mainly by a non-zero dipole moment. No data exist for these transitions either. Hence, theoretical calculations are

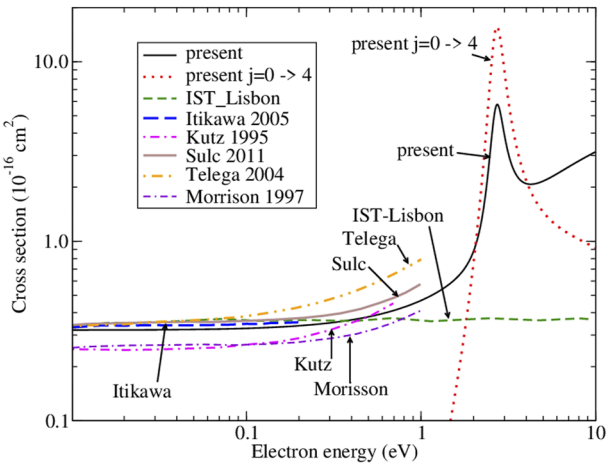

FIG. 8. Comparison of available cross sections of rotational excitation from the ground rotational level to $j = 2$ and $j = 4$. All curves, except the one explicitly marked with $0 \rightarrow 4$, correspond to the transition $j = 0 \rightarrow 2$. The recommended cross sections are the ones marked with "present."

also needed for these transitions, which are also expected to have small cross sections.

2.5. Vibrational excitation cross sections

In the recent review by Itikawa,[26] the recommended cross section for vibrational excitation $v = 0 \rightarrow 1$ is combined from different beam experiments by Sohn *et al.*[55] below 1 eV, by Brennan *et al.*[57] and Sun *et al.*[39] for energies 1.5–5 eV, and by Tanaka, Yamamoto, and Okada[76] for energies 7.5–30 eV. The uncertainty of the recommended cross section was estimated to be 30%.

In 2014, Laporta *et al.*[77] published an excellent theoretical study on resonant vibrational excitation of N_2. The calculations reproduced almost perfectly the complex $^2\Pi_g$ resonance structure of the experimental cross sections measured previously by Allan[45] and Vićić, Poparic, and Belić.[78] The calculations were performed for transitions between all 59 vibrational levels of the ground electronic state of N_2 for several values of the rotational angular momentum, while the rotational structure of the initial and final vibrational levels was neglected. Computed cross sections are provided as the supplementary material in the original article[77] and in this paper. Figure 9 and Table 7 shows examples of the excitation cross sections obtained by Laporta *et al.*[77] and compared with the experiment.[45]

The uncertainty in the experimental data of Allan[45] is ±20%. The agreement between the theory[77] and experiment is within that uncertainty. It probably means that the uncertainty of the theoretical data, which is evaluated in the original study, is better than 20%.

In their study, Laporta *et al.*[77] also computed the rate coefficients for the vibrational excitation transitions and fitted the obtained results to an analytical formula [Eq. (10) of Ref. 77],

$$k_v(T) = k_v^{\max}\left(\frac{T_v^{\max}}{T}\right)^{3/2} \exp\left(-\frac{T_v^{\max}}{T}\right), \qquad (2)$$

TABLE 6. Recommended cross sections of rotational excitation from the ground rotational level to $j = 2$ and $j = 4$ of N_2 in the units of 10^{-16} cm^2. Energy in eV

Electron energy (eV)	RECS ($j = 0 \rightarrow 2$) (10^{-16} cm^2)	Electron energy (eV)	RECS ($j = 0 \rightarrow 4$) (10^{-16} cm^2)
0.01	0.320	0.01	0.004
0.23	0.342	0.23	0.004
0.45	0.372	0.45	0.005
0.67	0.407	0.67	0.007
0.89	0.447	0.89	0.013
1.12	0.492	1.12	0.027
1.34	0.545	1.34	0.060
1.56	0.611	1.56	0.136
1.78	0.707	1.78	0.315
2.00	0.882	2.00	0.767
2.10	1.029	2.10	1.199
2.21	1.264	2.21	1.928
2.31	1.663	2.31	3.194
2.41	2.362	2.41	5.425
2.52	3.525	2.52	9.095
2.62	4.993	2.62	13.580
2.72	5.772	2.72	15.651
2.83	5.326	2.83	13.808
2.93	4.441	2.93	10.713
3.03	3.695	3.03	8.171
3.14	3.172	3.14	6.389
3.24	2.818	3.24	5.167
3.34	2.579	3.34	4.313
3.45	2.413	3.45	3.697
3.55	2.298	3.55	3.241
3.66	2.218	3.66	2.893
3.76	2.162	3.76	2.622
3.86	2.124	3.86	2.407
3.97	2.099	3.97	2.232
4.07	2.085	4.07	2.089
4.17	2.078	4.17	1.969
4.28	2.077	4.28	1.868
4.38	2.080	4.38	1.782
4.48	2.088	4.48	1.708
4.59	2.099	4.59	1.644
4.69	2.112	4.69	1.588
4.79	2.127	4.79	1.538
4.90	2.144	4.90	1.495
5.00	2.163	5.00	1.455
5.56	2.275	5.56	1.302
6.11	2.399	6.11	1.204
6.67	2.523	6.67	1.135
7.22	2.642	7.22	1.083
7.78	2.756	7.78	1.040
8.33	2.863	8.33	1.005
8.89	2.964	8.89	0.973
9.44	3.058	9.44	0.945
10.00	3.151	10.00	0.919

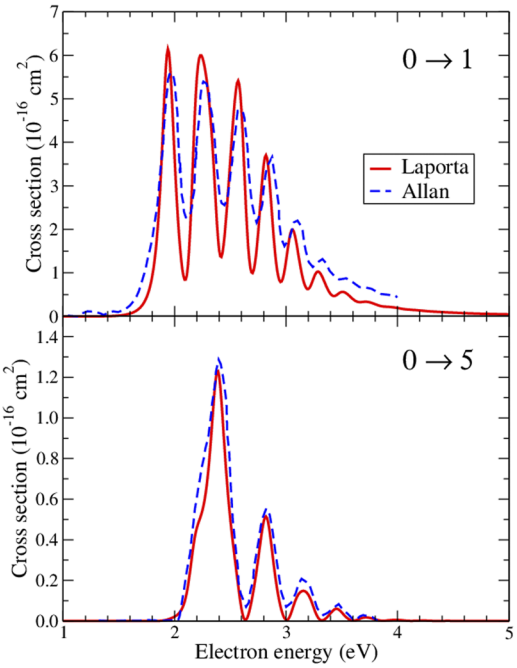

FIG. 9. Examples of theoretical[77] and experimental[45] cross sections for vibrational excitation $v = 0 \rightarrow 1$ (upper panel) and 5 (lower panel).

with the fitting parameters $k_v^{\max}$ and $T_v^{\max}$ provided. The fitting parameters are also given in the supplementary material of their study.[77]

In this paper, we recommend the theoretical data by Laporta *et al.*,[77] the cross sections and the rate coefficients, for the vibrational excitation. The cross sections and fitting parameters for the rate coefficients for transitions between the lowest 59 vibrational levels are provided in the supplementary material. The uncertainty of the cross sections, at least, for the lowest vibrational levels, is better than ±20% for energies above 1 eV. The uncertainty in the rate coefficients is much better, probably, below 5% for temperatures above 10 000 K (Fig. 10).

2.6. Electronic excitation cross section

Due to their importance in atmospheric processes, electronic excitations of the ground N_2 $X\ ^1\Sigma_g^+$ state have been extensively studied. Four methodologies are used: theory, optical emission measurements, analysis of swarm experiments,[79,80] and direct electron scattering, i.e., electron energy-loss (EEL) measurements. Among recent theoretical approaches, we mention R-matrix calculations by Gillan *et al.*[81] and by Tashiro and Morokuma[82] and the Schwinger multichannel calculations by Da Costa and Lima.[83] Recently, Su *et al.*[84,85] used the UK molecular R-matrix codes to perform a comprehensive study of electronic excitation from the ground state as well as the metastable $A\ ^3\Sigma_u^+$ and $a\ ^1\Pi_u$ excited states of the molecule to the eight lowest electronic states: $A\ ^3\Sigma_u^+$, $B\ ^3\Pi_g$, $W\ ^3\Delta_u$, $B'\ ^3\Sigma_u^-$, $a\ ^1\Pi_g$, $a'\ ^1\Sigma_u^-$, $w\ ^1\Delta_u$, and $C\ ^3\Pi_u$.

The recent experimental and theoretical cross sections for excitation of these states, as well as data from previous reviews,[26,28] are shown in Figs. 11–18. Threshold energies calculated by Su *et al.*[84] are given in Table 8. These energies agree well with the values derived from optical experiments by Oddershede *et al.*[86] but are somewhat higher—by about 1.5–1.9 eV for all the eight states, except $C\ ^3\Pi_u$—than the values from the EEL (i.e., beam) experiment[87] (see the last column in Table 8). Nuclear motion effects or the presence of the incoming projectile can lower the threshold for electron-impact electronic excitation.

The studies of optical emission[86] are simpler than EEL, but bigger uncertainties derive from normalization procedures and possible cascading processes; see, for example, the recent decomposition of the FUV spectrum (Lyman–Birge–Hopfield band system) due to the cascade de-excitation of the $a^1\Pi_g$ state by Ajello *et al.*[14]

Systematic studies of electronic excitation via beam experiments were performed by two laboratories: California State University[89,90] and Adelaide University.[91] Several sources of systematic uncertainties may arise in such measurements: the deconvolution of the EEL spectra in order to derive single vibronic (v') states, the normalization of the measured DCS due to unknown gas pressure and the geometry of the overlapping electron and gas beams, and the extrapolation (and integration) of DCS to obtain ICS. The current better understanding of the uncertainties in such experiments allows us to use earlier DCS[87,89] to derive more reliable ICS. For the California measurements, the most recent ICSs reported are those by Johnson *et al.*[88] for the eight states, mentioned above, for 10–100 eV collision energies, by Malone *et al.*[92] for the $C\ ^3\Pi_u$, $E\ ^3\Sigma_g^+$ and $a''\ ^1\Sigma_g^+$ states, and by Malone *et al.*[92] for higher states: $b\ ^1\Pi_u$, $c\ ^1\Pi_u$, $o_3\ ^1\Pi_u$, $b'\ ^1\Sigma_u^+$, $c_4'\ ^1\Sigma_u^+$, $G\ ^3\Pi_u$, and $F\ ^3\Pi_u$ for 17.5–100 eV collision energies. For the Adelaide group, the re-analyzed ICSs at 15–50 eV collision energy for ten states ($A\ ^3\Sigma_u^+$, $B\ ^3\Pi_g$, $W\ ^3\Delta_u$, $B'\ ^3\Sigma_u^-$, $a\ ^1\Pi_g$, $a'\ ^1\Sigma_u^-$, $w\ ^1\Delta_u$, $C\ ^3\Pi_u$, $E\ ^3\Sigma_g^+$, and $a''\ ^1\Sigma_g^+$) were published by Campbell *et al.*[91] The agreement between the results from the two laboratories is fairly good—within their combined error bars.

For optically allowed states, it is possible to extrapolate ICS up to higher collision energies using the Born-scaled approximation (see the work of Tanaka *et al.*[93]). The input parameter for such scaling is the generalized oscillator strength,[94] which can be obtained experimentally from high-energy x-ray scattering[95] or from near-to-zero angle DCS at high collision energies. Such a study, at 1500 eV collision energy and 12.4–13.3 eV energy loss, was recently made by Liu *et al.*[96] They resolved four vibronic levels of the $b\ ^1\Pi_u$ state, derived the generalized oscillator strength, and calculated ICS using the Born scaling: the agreement with the ICS measurements by Malone *et al.*[90] is good.

Numerous reviews[28,61,97] gave recommended cross sections. Itikawa[26] reported the "preferred" ICSs for ten states from the review by Buckman, Brunger, and Elford;[63] those, in turn, were obtained as weighted values from earlier experiments and calculations. Kawaguchi, Takahashi, and Satoh[28] [41] gave recommended ICS from energies up to 10 keV for 17 states using the recent EEL (i.e., electron beam) sets of ICS from the California laboratory.[90] Those recommended sets by Itikawa,[26] Kawaguchi, Takahashi, and Satoh[28] are shown in Figs. 11–18. In the present paper, we recommend the most recent data obtained theoretically by Su *et al.*,[84]

TABLE 7. Recommended cross sections of vibrational excitation from the ground rotational level to $v = 1$ of N_2 in the units of 10^{-16} cm^2. Energy in eV

El. energy (eV)	VECS $v = 0 \rightarrow 1$ (10^{-16} cm^2)	El. energy (eV)	VECS $v = 0 \rightarrow 1$ (10^{-16} cm^2)	El. energy (eV)	VECS $v = 0 \rightarrow 1$ (10^{-16} cm^2)
1.00	0.001 89	2.34	3.827	3.68	0.3309
1.03	0.001 64	2.37	2.616	3.71	0.3360
1.05	0.001 39	2.40	1.624	3.74	0.3302
1.08	0.001 15	2.42	1.392	3.77	0.3124
1.11	0.000 90	2.45	1.885	3.79	0.2874
1.13	0.000 67	2.48	2.747	3.82	0.2611
1.16	0.000 47	2.50	3.719	3.85	0.2398
1.19	0.000 30	2.53	4.657	3.87	0.2272
1.21	0.000 19	2.56	5.308	3.90	0.2217
1.24	0.000 16	2.58	5.250	3.93	0.2176
1.27	0.000 25	2.61	4.210	3.95	0.2109
1.30	0.000 49	2.64	2.656	3.98	0.2011
1.32	0.000 94	2.66	1.479	4.01	0.1890
1.35	0.001 68	2.69	1.009	4.03	0.1767
1.38	0.002 81	2.72	1.170	4.06	0.1661
1.40	0.004 44	2.74	1.783	4.09	0.1585
1.43	0.006 76	2.77	2.658	4.11	0.1530
1.46	0.010 0	2.80	3.460	4.14	0.1481
1.48	0.014 5	2.83	3.664	4.17	0.1426
1.51	0.020 7	2.85	3.095	4.19	0.1364
1.54	0.029 2	2.88	2.154	4.22	0.1298
1.56	0.040 9	2.91	1.354	4.25	0.1233
1.59	0.057 0	2.93	0.894	4.28	0.1176
1.62	0.079 5	2.96	0.802	4.30	0.1129
1.64	0.111 1	2.99	1.056	4.33	0.1088
1.67	0.155 6	3.01	1.518	4.36	0.1049
1.70	0.220 0	3.04	1.917	4.38	0.1010
1.72	0.314 6	3.07	1.959	4.41	0.0970
1.75	0.455 3	3.09	1.671	4.44	0.0930
1.78	0.671 4	3.12	1.262	4.46	0.0892
1.81	1.013	3.15	0.9046	4.49	0.0858
1.83	1.558	3.17	0.6837	4.52	0.0827
1.86	2.430	3.20	0.6328	4.54	0.0798
1.89	3.748	3.23	0.7474	4.57	0.0771
1.91	5.288	3.26	0.9265	4.60	0.0744
1.94	6.138	3.28	1.0255	4.62	0.0717
1.97	5.473	3.31	0.9826	4.65	0.0692
1.99	4.031	3.34	0.8459	4.68	0.0668
2.02	2.659	3.36	0.6862	4.70	0.0645
2.05	1.651	3.39	0.5516	4.73	0.0624
2.07	1.019	3.42	0.4772	4.76	0.0604
2.10	0.853	3.44	0.4749	4.79	0.0585
2.13	1.428	3.47	0.5207	4.81	0.0566
2.15	2.879	3.50	0.5583	4.84	0.0548
2.18	4.622	3.52	0.5536	4.87	0.0531
2.21	5.709	3.55	0.5111	4.89	0.0515
2.23	5.997	3.58	0.4497	4.92	0.0499
2.26	5.828	3.60	0.3893	4.95	0.0485
2.29	5.415	3.63	0.3452	4.97	0.0471
2.32	4.774	3.66	0.3279	5.00	0.0457

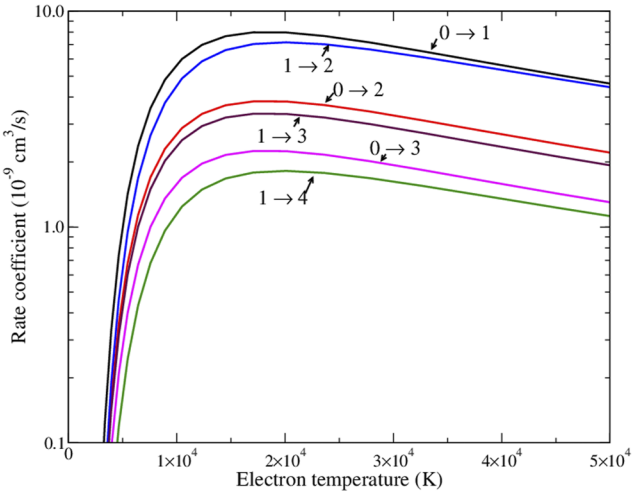

FIG. 10. Example of theoretical rate coefficients for vibrational excitation computed by Laporta *et al.*[77]

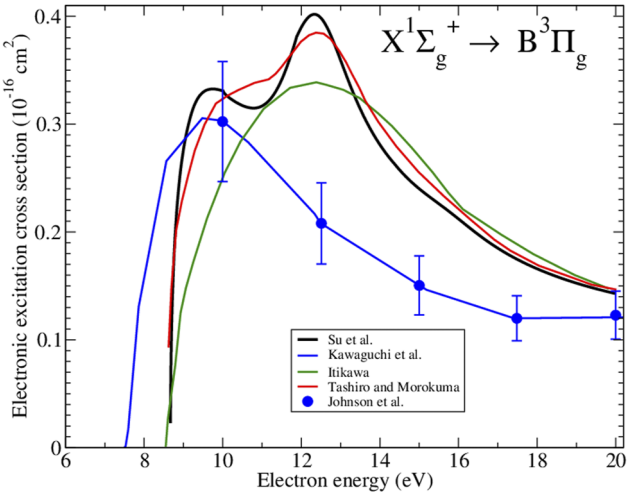

FIG. 12. Cross section for excitation of the $B^3\Pi_g$ electronic state from the ground state: Black thick line—Su *et al.*[84] (recommended in this paper), blue line—Kawaguchi, Takahashi, and Satoh,[28] green solid line—Itikawa,[26] red line—Tashiro and Morokuma,[82] and circle—Johnson *et al.*[88]

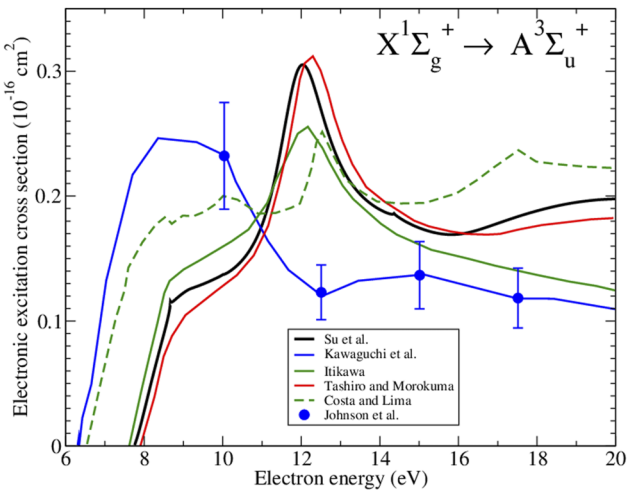

FIG. 11. Cross section for excitation of the $A^3\Sigma_u^+$ electronic state from the ground state: Black thick line—Su *et al.*[84] (theory, recommended in this paper), blue line—Kawaguchi, Takahashi, and Satoh[28] (review), green solid line—Itikawa[26] (review), red line—Tashiro and Morokuma[82] (theory), green dashed line—Da Costa and Lima[83] (theory), and circles—Johnson *et al.*[88] (experiment).

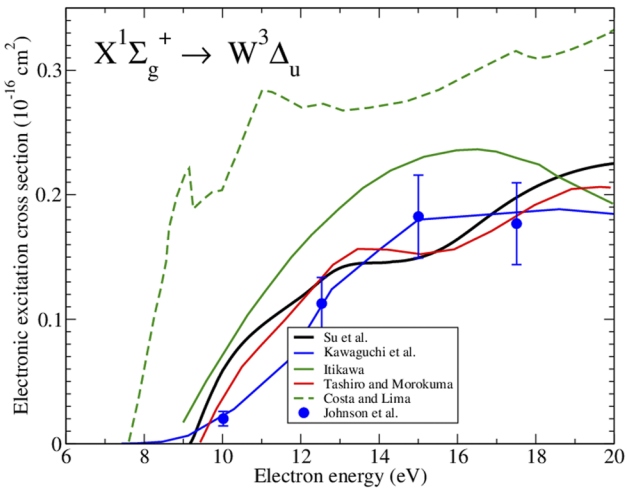

FIG. 13. Cross section for excitation of the W $^3\Delta_u$ electronic state from the ground state: Black thick line—Su *et al.*[84] (recommended in this paper), blue line—Kawaguchi, Takahashi, and Satoh,[28] green solid line—Itikawa,[26] red line—Tashiro and Morokuma,[82] green dashed line—Da Costa and Lima,[83] and circles—Johnson *et al.*[88]

shown by black lines in the figures, which agree fairy well with the majority (but not all) of the recent data (theory, experiment, and review) for the transitions, presented in the figures.

The recommended data presented in Figs. 11–18 are also provided in the supplementary material of this article.

2.7. Dissociation into neutrals

The triple molecular bond in N_2 is one of the strongest in chemistry, so the dissociation energy is high, 9.75 eV (see Refs. 100–102). Production of atomic nitrogen, either via dissociative ionization [see Eq. (7)], or via the dissociation into neutrals [Eq. (3)],

$$N_2 + e \rightarrow 2N + e, \tag{3}$$

is an important channel in Earth's (and Titan's[18]) atmospheric chemistry and in shock plasmas related to space shuttles.[103]

The determination of the threshold energy for the dissociation into neutrals via collision with electrons dates to 1956. Frost and

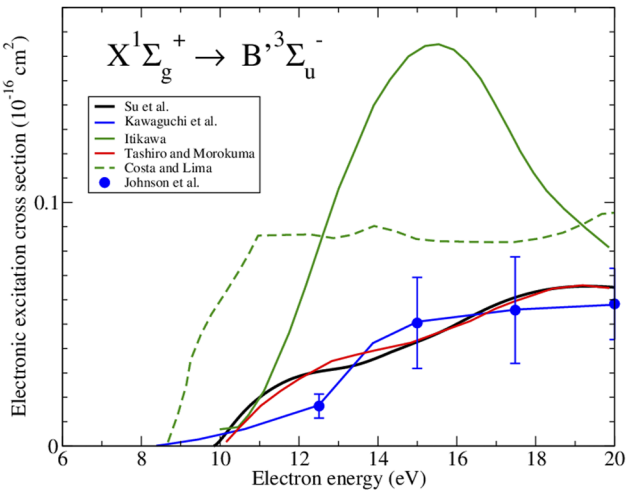

FIG. 14. Cross section for excitation of the B′ $^3\Sigma_u^-$ electronic state from the ground state: Black thick line—Su *et al.*[84] (recommended in this paper), blue line—Kawaguchi, Takahashi, and Satoh,[28] green solid line—Itikawa,[26] red line—Tashiro and Morokuma,[82] green dashed line—Da Costa and Lima,[83] and circles—Johnson *et al.*[88]

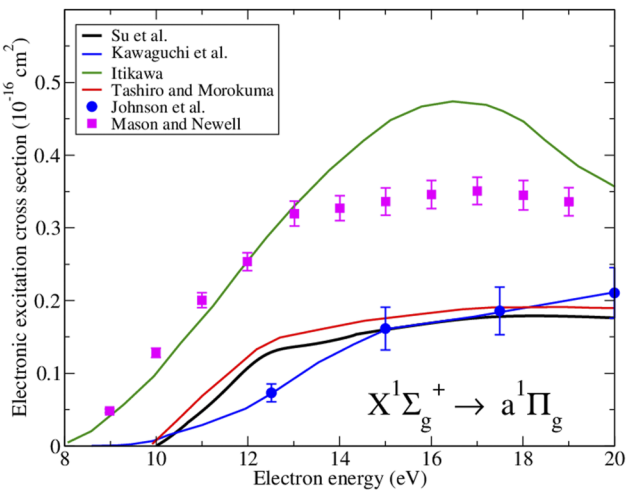

FIG. 15. Cross section for excitation of the a $^1\Pi_g$ electronic state from the ground state: Black thick line—Su *et al.*[84] (recommended in this paper), blue line—Kawaguchi, Takahashi, and Satoh,[28] green solid line—Itikawa,[26] red line—Tashiro and Morokuma,[82] circles—Johnson *et al.*,[88] and squares—Mason and Newell.[98]

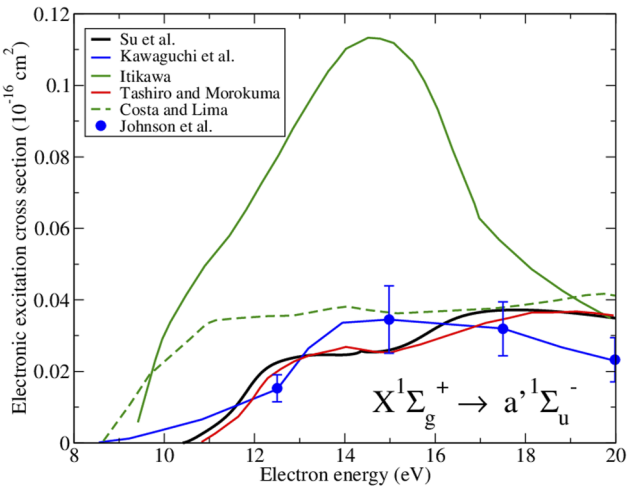

FIG. 16. Cross section for excitation of the a′ $^1\Sigma_u^-$ electronic state from the ground state: Black thick line—Su *et al.*[84] (recommended in this paper), blue line—Kawaguchi, Takahashi, and Satoh,[28] green solid line—Itikawa,[26] red line—Tashiro and Morokuma,[82] green dashed line—Da Costa and Lima,[83] and circles—Johnson *et al.*[88]

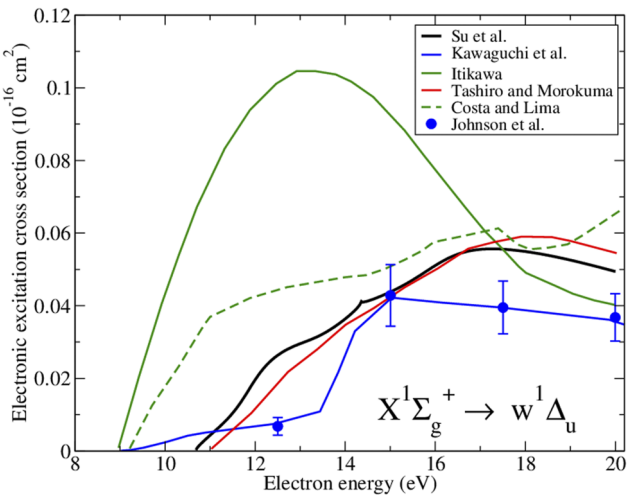

FIG. 17. Cross section for excitation of the *w* $^1\Delta_u$ electronic state from the ground state: Black thick line—Su *et al.*[84] (recommended in this paper), blue line—Kawaguchi, Takahashi, and Satoh,[28] green solid line—Itikawa,[26] red line—Tashiro and Morokuma,[82] green dashed line—Da Costa and Lima,[83] and circles—Johnson *et al.*[88]

McDowell[100] studied the ion current above the threshold for the dissociative ionization [see Eq. (7)]; from changes in the slope of the ion-yield curve, they deduced openings of different channels. They concluded that the N^+ ion is produced always in the ^{3}P state, while the N atom is produced in ^{4}S, ^{2}D, and ^{2}P states, with rising threshold, respectively.

The dissociation-into-neutral channels and relative thresholds are[101]

$$N_2 \rightarrow N(^4S) + N(^4S) \quad (9.75\ \text{eV}), \tag{4}$$

$$N_2 \rightarrow N(^2D) + N(^4S) \quad (12.14\ \text{eV}), \tag{5}$$

$$N_2 \rightarrow N(^2P) + N(^4S) \quad (13.33\ \text{eV}). \tag{6}$$

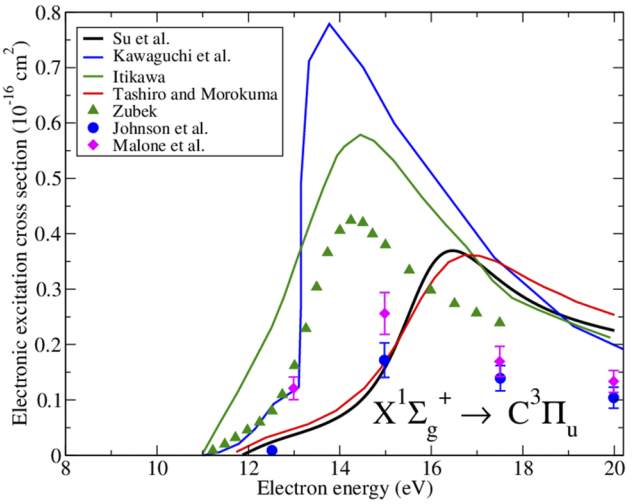

FIG. 18. Cross section for excitation of the $C\,^3\Pi_u$ electronic state from the ground state: Black thick line—Su *et al.*[84] (recommended in this paper), blue line—Kawaguchi, Takahashi, and Satoh,[28] green solid line—Itikawa,[26] red line—Tashiro and Morokuma,[82] triangles—Zubek,[99] circles—Johnson *et al.*,[88] and diamonds—Malone *et al.*[92]

TABLE 8. Threshold energies (to $v' = 0$), in eV, for excitation of the eight low-laying electronic states in N_2. (a) Vertical excitation energies in calculation of Su *et al.*[84] obtained using the 6-311G** basis set. (b) Experimental excitation energies as evaluated by Oddershede *et al.*[86] from optical measurements. (c) Excitation energies from EEL spectrum measurements[87]

Target state	Theory[84]	Expt.[86]	Expt.[87]
$X\ ^1\Sigma_g^+$	−109.1027		
$A\ ^3\Sigma_u^+$	7.78	7.75	6.169
$B\ ^3\Pi_g$	8.64	8.04	7.353
$W\ ^3\Delta_u$	9.20	8.88	7.362
$B'\ ^3\Sigma_u^-$	9.88	9.67	8.549
$a\ ^1\Pi_g$	10.00	9.31	8.549
$a'\ ^1\Sigma_u^-$	10.46	9.92	8.398
$w\ ^1\Delta_u$	10.75	10.27	8.895
$C\ ^3\Pi_u$	11.85	11.19	11.032

Out of the atomic states formed, the ^2D_J state is particularly long-lived, with radiative lifetimes of 17 and 40 h, for the $J = 3/2$ and $J = 5/2$ components, respectively.[104] Winters[105] evaluated the total absolute dissociation cross section for electron energies from 0 to 300 eV. He measured the quantity of nitrogen atoms adsorbed on nickel and molybdenum surfaces. By subtracting the cross section for the dissociative ionization [i.e., essentially for the process (8)] of Rapp and Englander-Golden[106] from the total N signal (open triangles in Fig. 19), one can evaluate the cross section for the dissociation into neutrals, Eq. (3) (see closed triangles in Fig. 19). An estimated uncertainty of these values is ±20%.

Cosby[101] used a collimated beam of N_2 molecules created by near-resonant charge transfer neutralization of the N_2^+ beam. Dissociated fragments were detected by a position-sensitive detector.

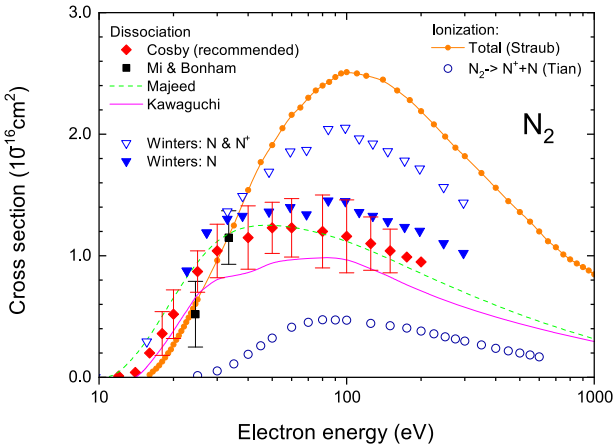

FIG. 19. Overview of the experimental determinations of the dissociation into neutral ($N_2 \rightarrow 2N$) cross section. The recommended values are these given by Cosby (diamonds with error bars). Winters measured[105] the deposition of N atoms in the vacuum tube: Open triangles is the summed cross section for the formation of N and N^+ fragments; the cross section for the neutral dissociation (closed triangles) may be obtained by subtracting the cross section for the dissociative ionization from these summed values. Here, we used the cross sections by Tian and Vidal[109] for the ionization into the (N^+ and N) channel (open circles) and into the ($N^+ + N^+$) channel (not shown). The two determinations (by Cosby[101] and by Winters[105]) agree within error bars; in addition, the dissociation cross section by Mi and Bonham[108] in the threshold region falls within these bars. Values recommended by Kawaguchi, Takahashi, and Satoh[28] and Majeed and Strickland[110] are shown as broken and solid curves, respectively. The total ionization cross section[111] is shown for comparison.

The uncertainty varied from 60% at 18.5 eV to 30% at higher energies. The intrinsic difficulty of this method comes from the need to account for the dissociative ionization and for the dissociation of the excited metastable ions present in the beam. The results of Cosby are 30%–50% lower than those by Winters;[105] however, the two sets overlap within the combined uncertainties.

Additional comparison may be made with measurements of optical emission due to electron impact.[107] Several electronically excited states are situated above the thresholds for dissociation, so the dissociation process competes with the fluorescence. Using dissociation probabilities of seven electronically excited states and the optical emission cross sections from these states,[107] one obtains cross sections for dissociation as high as 0.6×10^{-16} cm^2 at 200 eV. From all these considerations, Cosby[101] recommended weighted averages in-between his and Winter's data: They are shown in Fig. 19 with uncertainties given by Cosby. From measurements of translational energies, Cosby concluded that at 48.5 eV, the dominant dissociation pattern is $N_2 \rightarrow N\ (^2D) + N(^4S)$; the same translational energy spectrum excludes any significant production of the $N(^4S) + N(^4S)$ dissociation products.

Mi and Bonham,[108] using two time-of-flight tubes working in coincidence, measured elastic, total inelastic, ionization, and dissociation plus excitation cross sections at 24.5 and 33.4 eV. Their dissociation cross section agrees within the uncertainties with the data by Cosby (see Fig. 19).

The recent reviews by Majeed and Strickland[110] and Itikawa[26] used the recommended cross sections by Cosby;[101] Kawaguchi,

Takahashi, and Satoh[28] recommended somewhat lower values (see Fig. 19). We also recommend the Cosby set (see Table 9); an uncertainty of ±20% is associated with these values. The maximum of the dissociation cross sections is 1.2×10^{-16} cm^2 at 80 eV. At 100 eV, the cross section is half of the total ionization (see Fig. 19), meaning that neutral atoms play an important role in nitrogen plasmas.[7]

2.8. Ionization cross section

Three generations of methods have been applied to measure ionization cross sections: (i) Those collecting the total ion current as used by Rapp and Englander-Golden,[106] i.e., measuring the gross total ionization, (ii) those using mass spectrometers (magnetic field,[112,113] quadrupole Halas and Adamczyk,[114] Crowe and McConkey,[115] Krishnakumar and Srivastava,[116] and time-of-flight[109]) to select ions produced; (iii) and the most recent setups[111,117,118] using position-sensitive detectors to determine also coincidences and the energy distribution of ions.

Due to the importance of nitrogen ions in plasma and atmospheric chemistry, numerous reviews give ionization cross sections.[26,28,109] Itikawa[26] recommended the same set of total and partial ionization cross sections as Lindsay and Mangan[119] did. We show these data in Fig. 20.

Generally, the agreement between the different methods for the total ionization cross section is within a 10% spread (see Fig. 21). The recommended data, based on measurements by Straub *et al.*,[111] were somewhat lowered in their maximum by Lindsay and Mangan[119] due to the improved analysis of the experiment.[111] In the energy range from threshold to 25 eV, Lindsay and Mangan[119] recommended data by Rapp and Englander-Golden[106] that cover more energy points and perfectly overlap with those by Stebbings and Lindsay[120] at higher energies. In the high energy limit, the data of Rapp and Englander-Golden[106] are somewhat overestimated due to a non-complete collecting of the incident electron beam. Krishnakumar and Srivastava[116] used the relative-flow method for normalization, which introduced additional uncertainties. The most recent set by Shen *et al.*[118] in the 250–8000 eV merges smoothly with the recommended data, while observed differences can to be attributed to normalization procedures[118] to three different Ar^+ measurements in three energy ranges, in particular, to that by Schram *et al.*[112] above 1000 eV. The recommended total ionization

TABLE 9. Recommended dissociation cross sections of N_2 in the units of 10^{-16} cm^2. Energy in eV

Electron energy (eV)	N + N (10^{-16} cm^2)
12	0.01
14	0.04
16	0.2
18	0.36
20	0.52
25	0.87
30	1.04
40	1.15
50	1.23
60	1.23
80	1.2
100	1.16
125	1.1
150	1.04
175	0.99
200	0.95

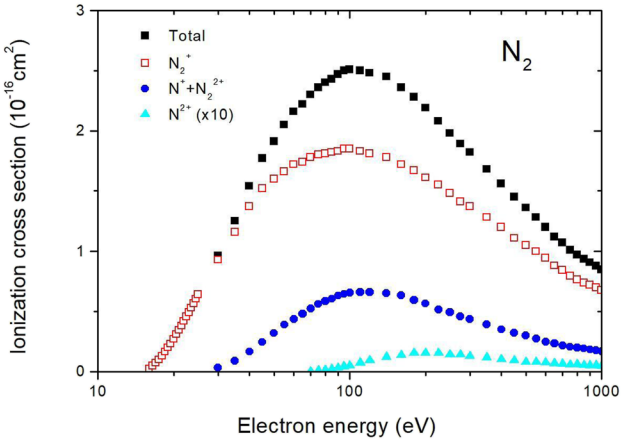

FIG. 20. Recommended total and partial ionization cross sections. These data are based on the review of Lindsay and Mangan.[119]

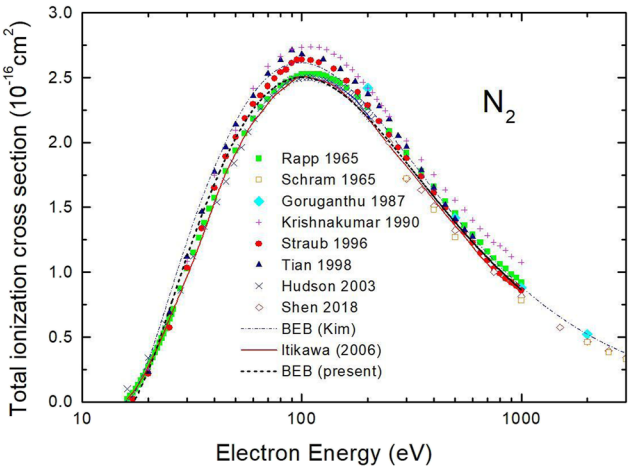

FIG. 21. Comparison of total ionization cross sections of N_2. Present recommended values follow those given by Lindsay and Mangan,[119] based on re-analyzed measurements of Straub *et al.*[111] In the low energy range, the recommended set is closer to the early result of Rapp and Englander-Golden[106] while at high energies closer to the data by Straub *et al.* The same set was recommended by Itikawa,[26] red thick line. Symbols are green full squares, Ref. 106; orange open squares, Ref. 112; cyan full diamonds, Ref. 121; magenta crosses, Ref. 116; red circles, Ref. 111; black triangles, Ref. 109; blue crosses, Ref. 122; and red open diamonds, Ref. 118. BEB (Born-Bethe binary-collisions model) model: Blue dashed-dotted line, Ref. 123; black thick broken line, present calculation (see Table 10 for the orbital parameters used). Data of Märk[113] (not shown) are in the whole energy range (i.e., up to 165 eV) lower than the recommended value (by 10% at 100 eV).

TABLE 10. Recommended total and partial ionization cross sections of N_2 in the units of 10^{-16} cm^2. Energy in eV

Energy	σ (N_2^+)	σ ($N^+ + N_2^{2+}$)	σ (N^{2+})	σ (total)
16.0	0.0211			0.0211
16.5	0.0466			0.0466
17.0	0.0713			0.0713
17.5	0.0985			0.0985
18.0	0.129			0.129
18.5	0.164			0.164
19.0	0.199			0.199
19.5	0.230			0.230
20.0	0.270			0.270
20.5	0.308			0.308
21.0	0.344			0.344
21.5	0.380			0.380
22.0	0.418			0.418
22.5	0.455			0.455
23.0	0.492			0.492
23.5	0.528			0.528
24.0	0.565			0.565
24.5	0.603			0.603
25	0.640			0.640
30	0.929	0.0325		0.962
35	1.16	0.0904		1.25
40	1.37	0.166		1.54
45	1.52	0.245		1.77
50	1.60	0.319		1.91
55	1.66	0.39		2.05
60	1.72	0.438		2.16
65	1.74	0.482		2.22
70	1.78	0.523	0.001 71	2.30
75	1.80	0.561	0.006 58	2.36
80	1.81	0.587	0.012 2	2.40
85	1.82	0.605	0.020 4	2.43
90	1.83	0.632	0.032 8	2.47
95	1.85	0.645	0.043 9	2.50
100	1.85	0.656	0.049 5	2.51
110	1.83	0.66	0.072 5	2.50
120	1.81	0.661	0.092 7	2.48
140	1.78	0.652	0.122	2.45
160	1.72	0.633	0.137	2.36
180	1.67	0.595	0.154	2.28
200	1.61	0.566	0.154	2.19
225	1.55	0.516	0.154	2.08
250	1.48	0.493	0.142	1.98
275	1.41	0.458	0.141	1.89
300	1.37	0.438	0.128	1.82
350	1.28	0.393	0.117	1.68
400	1.20	0.351	0.103	1.56
450	1.11	0.324	0.094	1.45
500	1.05	0.299	0.080 8	1.36
550	0.998	0.274	0.079 6	1.28
600	0.943	0.248	0.076	1.20
650	0.880	0.234	0.070 1	1.12
700	0.844	0.217	0.064 9	1.07
800	0.765	0.2	0.059 4	0.971
850	0.738	0.192	0.054 3	0.936
900	0.719	0.183	0.052 2	0.907
950	0.698	0.176	0.050 5	0.879
1000	0.676	0.167	0.048 5	0.847

cross sections are given in Table 10 with an estimated uncertainty of 5%.

At 100 eV, the production of the parent N^{2+} ion dominates, amounting to 74% of the total ionization cross section (see Fig. 20). Good agreement (within 10%) is apparent between the more recent measurements[109,111,116,124] (see Fig. 22); earlier experiments[106,114,115] also overlap with the latter within error bars. The recommended values (with ±5% uncertainty) for the productions of the N^{2+} ion are given in Table 10. Doering *et al.*[125–128] measured the energy and angular distributions of the N_2^+ ion and concluded that at 100 eV, the branching ratio between the ground state of the N_2^+ ion ($X\,^2\Sigma_g^+$) and the two excited metastable states ($A\,^2\Pi_u$ and $B\,^2\Sigma_u^+$, located 1.118 and 3.170 eV above the X state) are 0.45:0.45:0.1 In other words, the N_2^+ ions are predominantly produced in the electronically excited states. Abramzon, Siegel, and Becker[129,130] used laser-induced fluorescence to identify the electronic states of N_2^+ produced in the energy region from threshold to 100 eV. They normalized the cross section to the branching ratio by Doering and Yang.[126] Figure 22 shows their cross

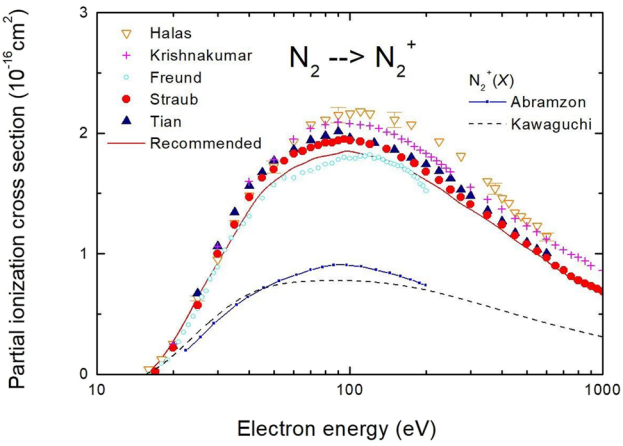

FIG. 22. Partial ionization cross section for the production of N_2^+ ion. Freund, Wetzel, and Shul[124] (cyan open circles) measured both the N_2^+ production from N_2 in its ground and from the metastable states. Other symbols are the same as in Fig. 21. Data of Rapp and Englander-Golden[106] and of Crowe and McConkey,[115] not shown, overlap with other sets within experimental uncertainties. The lower set of two curves is the cross section for the production of the N_2^+ ion in its electronically ground ($X\,^2\Sigma_g^+$) state. The data used by Kawaguchi *et al.*[28] are lower in their maximum than measurements of Abramzon *et al.*,[129] but at higher energies, they follow the same (45%) branching ratio.

sections for the production of N_2^+ in the ground ($X\ ^2\Sigma_g^+$) state. In the whole energy range up to 200 eV, only 45% of N_2^+ ions are produced in the ground state.

The second most abundant ion in the ionization of N_2 is N^+. In order to separate it (in traditional quadrupole mass spectrometers) from the N_2^{2+} dication, molecules consisting of two different isotopes, such as $^{15}N\ ^{14}N$, should be used. The N^+ ion can appear from three dissociative ionization processes (see, for example, the work of Tian and Vidal[109]),

$$e + N_2 \rightarrow N^+ + N + 2\,e - \text{ single}, \quad (7)$$

$$e + N_2 \rightarrow N^+ + N^+ + 3\,e - \text{ double}, \quad (8)$$

$$e + N_2 \rightarrow N^{2+} + N^+ + 4\,e - \text{ triple}. \quad (9)$$

Two methodologies—of the total ion current[106] and of the summed ions, in particular, in coincidence[111]—measure different cross sections: The gross total ionization and the counting total ionization, respectively. They differ significantly if multiple charged ions are abundant or when more than one ion are produced in the same event, such as in Eq. (8) (see also our paper on CH_4[32]). However, this does not seem be the case of N_2, as the gross total[106] and the counting total ionization cross sections coincide within experimental uncertainties.[120] Further arguments for it come from measurements of isotopically differentiated $^{15}N^{14}N$ molecules[114] and with position-sensitive detectors[109,122] (see below).

The agreement between different methodologies[109,111,116] on the total yield of ions (N^+ plus N_2^{2+}) is also very good (see Fig. 23). Even the data by Halas and Adamczyk[114] agree if we assume a plausible mistake in the normalization of different isotopes. Figure 23 also shows the measurements of the N_2^{2+} yield by Halas and Adamczyk[114] (using $^{15}N^{14}N$) and recent by results by Ferreira *et al.*[131] and Sigaud and Montenegro.[132] The agreement between the different methodologies is poor (see below), so we cannot give recommended values. Note that the analysis of electronic energies of the N_2^{2+} and N^+ ions indicates that the first one is metastable, so its detected yield may depend on details of the experimental techniques used. The cross section for production of the N_2^{2+} ion is ~1% of the total ionization cross section. The agreement[109,111,116] for the atomic dication N^{2+} is again very good: The yield of N^{2+} in its maximum (at 200 eV) is slightly less than 1% of the total ionization, as shown in Fig. 24.

Measurements in coincidence allow one to monitor separate channels of ionization, such as these in Eqs. (7) and (8). Tian and Vidal[109] measured total production of N_2^+ and N^+ ions, single ionization (N_2^+ and $N^+ + N$ channels), double ionization ($N^+ + N^+$ and $N^{2+} + N$ channels), and triple ionization ($N_2^+ + N$ channel, Fig. 24). The double ionization reaches a maximum of 0.14×10^{-16} cm^2 at about 125–140 eV, where it constitutes 6% of the total ionization cross section. This makes a 3% difference between the gross total and counting TCS, thus explaining the good agreement between different experimental methods.

Partitioning into separate ionization channels as measured by Tian and Vidal[109] is shown in Fig. 25; as seen from this figure, the single, double, and triple ionizations (thick lines in the figure) scale in their maxima by a factor of 20 roughly: This reflects rising threshold for these ionization processes. At high energies, the production of the N^+ ion in single ionization events, Eq. (7), is a factor of three more probable than in double ionization [Eq. (8)]. Note, however, also that even the same laboratories find difficulties in determining precise values of the channel-defined cross sections (compare, for example, results for the N_2^{2+} ion by Bull, Lee, and Vallance[117,133] and by Ferreira *et al.*[131] and Sigaud and Montenegro).[132]

Additional information on the dynamics of the ionization is deducible from kinetic energies of ions produced. For N_2^+ ions at 70 eV, Crowe and McConkey[115] observed a single broad peak in the ion kinetic energy around 2 eV, at 90 eV (a second, superimposed peak at 5 eV), and at 300 eV collision energy (an additional peak around 8 eV). This testifies to the opening of new ionization channels. Recent measurements[134] of the kinetic energy release using coincidence techniques try to attribute such peaks to individual molecular orbital.

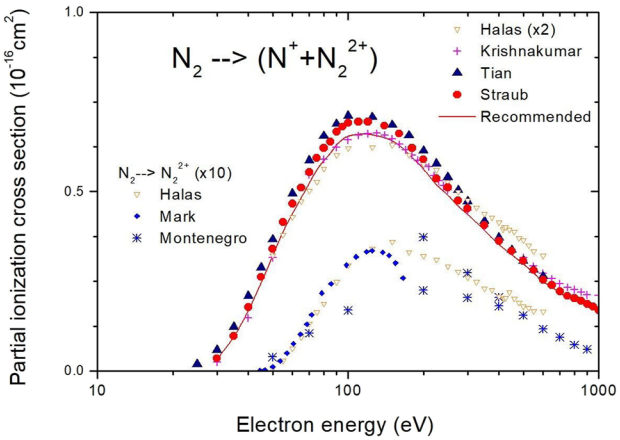

FIG. 23. Production of N^+ and N_2^{2+} ions. The two ions are indistinguishable in mass spectrometers, unless two different isotopes (i.e., $^{15}N\ ^{14}N$) like in Ref. 114 or position-sensitive detector[131] are used.

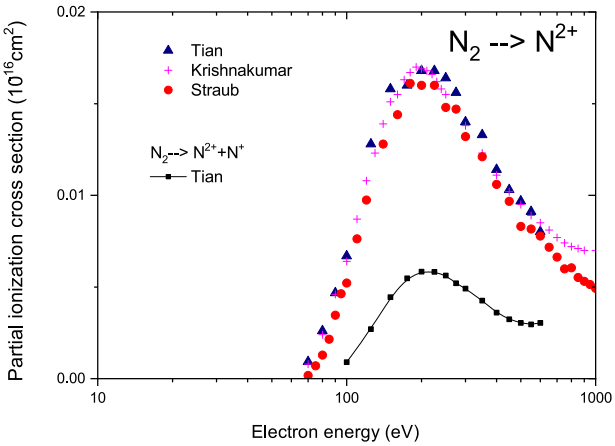

FIG. 24. Production of the N^{2+} atomic dication from N_2 (total yield). The lower curve is the distinction of the triple dissociative ionization events [Eq. (9)].

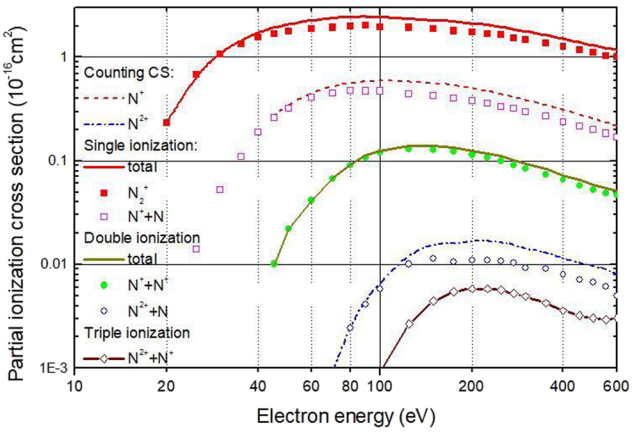

FIG. 25. Channel-resolved ionization cross sections of N_2—data by Tian and Vidal.[109] Thick lines, from the upper, are single, double, and triple ionizations—i.e., with the precursor ion N_2^+, N_2^{2+} and N_2^{3+}—respectively. Parent (N_2^+) ion production are red solid squares, magenta open squares are single dissociative ionization ($N^+ + N$), green solid circles are double symmetric ionization ($N^+ + N^+$), and blue open circles are ($N_2^+ + N$). In contrast to Table 1 by Tian and Vidal,[109] the N^+ production (the dashed line in the figure) is not the total ion current (i.e., the gross cross section) but the number of events leading to the formation of N^+ ion, i.e., the counting cross section. The blue dotted-dashed line is the counting cross section for the N^{2+} ion. Brown open diamonds, superimposed with the triple ionization, correspond to ($N^{2+} + N$).

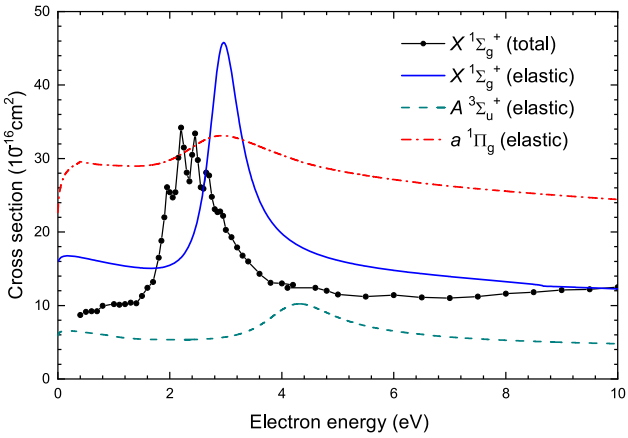

FIG. 26. Theoretical[84] cross sections for elastic electron scattering on N_2 in the ground $X\ ^1\Sigma_g^+$ and metastable $A\ ^3\Sigma_u^+$ and $a\ ^1\Pi_g$ states. Experimental TCSs for the N_2 molecule is also shown.

3. Metastable N_2^* Molecule

As discussed in Sec. 2.6, cross sections for electronic excitations in electron scattering on nitrogen molecule are relatively high, compared, for example, with the CH_4 molecule.[32] This is attributed to high thresholds for the dissociation into neutrals (9.75 eV) and ionization (15.58 eV).[135]

The lowest, triplet $A\ ^3\Sigma_u^+$ metastable state, with a threshold of 6.2 eV, has a lifetime close to 2.4 s.[7,18] The vibronic progression of de-excitation to this state ($B\ ^3\Pi_g \rightarrow A\ ^3\Sigma_u^+$, the so-called first positive band) dominates in the visible range in N_2 afterglows.[13] The metastable $a\ ^1\Pi_g$ state, with a threshold of 8.5 eV, is rather short-lived (56 μs radiative lifetime of $v = 0$–2 levels[136]) but at conditions of an electrical discharge may be quenched to the $a'\ ^1\Sigma_u^+$ state, with almost overlapping vibronic levels and with the lifetime of 20 ms.[137] De-excitation (and excitation) cross sections from excited states are needed to model nitrogen plasmas, the optical emission, in particular.[134]

3.1. Total, elastic and vibrational cross section

To our knowledge, no experiments on TCSs of metastable states of N_2 have been performed. Recently, Su *et al.*[85] using the R-matrix method (UKRMol+/QEC codes[74,75]) calculated integral elastic cross sections for electron scattering on N_2 being in the $A\ ^3\Sigma_u^+$ and $a\ ^1\Pi_g$ states for energies 0–10 eV. The integral elastic cross section for scattering on N_2 in the ground $X\ ^1\Sigma_g^+$ state was also computed. These three cross sections are shown in Fig. 26. For the ground state, the calculated elastic cross section is in apparent disagreement with our recommended values (see Sec. 2.2). Note, however, that the R-matrix method uses the fixed-nuclei approximation, i.e., nuclear motion of the molecule is neglected. If we compare the calculated[84] ICS for the $X\ ^1\Sigma_g^+$ state with the experimental TCS, the agreement is surprisingly good. Therefore, we deduce that also for the two metastable states, the calculation gives a good insight into the TCS.

The ICSs for the $A\ ^3\Sigma_u^+$ and $a\ ^1\Pi_g$ states show resonant maxima at energies close to the energy of the 2.4 eV shape resonance in the ground-state N_2 [4.2 and 3 eV, respectively, for the two metastables (see Fig. 26)]. The cross sections at these resonances are high, above 30×10^{-16} cm^2. One can expect that similarly to the 2.4 eV shape resonance for the ground-state N_2, the contribution from the vibrational excitation to the $A\ ^3\Sigma_u^+$ and $a\ ^1\Pi_g$ cross sections is high: Compare with Fig. 2 and recall that for the 2.4 eV shape resonance in the cross section for the ground state of N_2, the summed vibrational cross sections amount to about 1/3 of the TCS. Note also that in contrast to the $A\ ^3\Sigma_u^+$ state, the theoretical[84] integral elastic cross for the $a\ ^1\Pi_g$ state is high (above 24×10^{-16} cm^2) in the whole 0–10 eV energy range. Such a high cross section at low energies is quite exceptional for electron scattering, even on polyatomic molecules. The low-energy $^2\Pi$ resonance does not lead to dissociative electron attachment (DEA) as it is situated far below the N_2 dissociation energy. However, it is likely that the higher energy resonances found in the 10 eV region[84] will lead to DEA similarly to the isoelectronic CO system.[138]

3.2. Electronic excitation and de-excitation cross section

Recently, Su *et al.*[84] studied theoretically excitations and de-excitations between the lowest electronic states, namely, from $A\ ^3\Sigma_u^+$ and $a\ ^1\Pi_g$ to $X\ ^1\Sigma_g^+$, $a'\ ^1\Sigma_u^-$, $B\ ^3\Pi_g$, $B'\ ^3\Sigma_u^-$, $C\ ^3\Pi_u$, $W\ ^3\Delta_u$, and $w\ ^1\Delta_u$. The most unexpected result from these calculations is a resonant-like enhancement at low collision energies (2–4 eV), leading to large ICSs:

- 2.3×10^{-16} cm^2 for the $A\ ^3\Sigma_u^+ \rightarrow B\ ^3\Pi_g$ excitation (i.e., populating the first positive band optical transition), see Fig. 27;

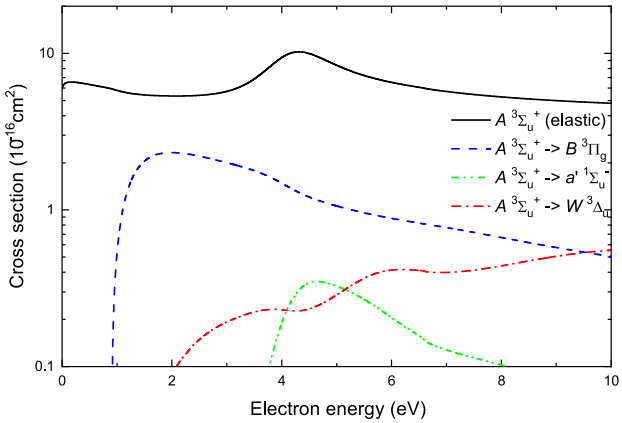

FIG. 27. Theoretical[84] cross sections for electronic excitation from the metastable $A\ ^3\Sigma_u^+$ state to the $B^3\Pi_g$, $a'^1\Sigma_u^-$ and $W^3\Delta_u$ states. Elastic cross section for $A\ ^3\Sigma_u^+$ is also shown.

- 0.35×10^{-16} cm^2 for the $A\ ^3\Sigma_u^+ \rightarrow a'\ ^1\Sigma_u^-$ transition between two metastable states that, in its turn, may change the apparent lifetimes in plasmas and afterglows, Fig. 28;
- 4.8×10^{-16} cm^2 at 0.8 eV for the resonant transition, $a\ ^1\Pi \rightarrow a'\ ^1\Sigma_u^-$, i.e., to the "iso-vibronic" metastable, with a much longer lifetime (see above);
- 3.1×10^{-16} cm^2 at 1.1 eV for the $a\ ^1\Pi \rightarrow w\ ^1\Delta_u$ transition (see Fig. 28), indirectly populating the second positive (C → B) optical band.

Note that detailed excitation and de-excitation cross sections for the transitions between the lowest eight electronic states of N_2 are available in the supplementary data by Su *et al.*[84]

Summarizing, the electronic transitions between excited states, in particular, excitations and resonant-like de-excitations of the metastables, significantly influence the dynamic of nitrogen discharges. Including these processes into modeling may solve long-standing "mysteries" in nitrogen plasmas and afterglows.[7]

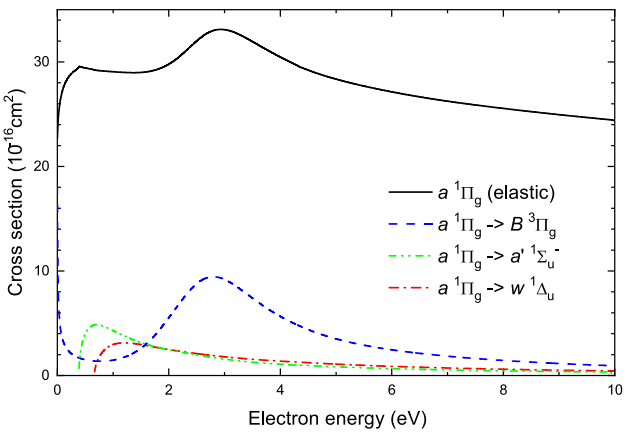

FIG. 28. Theoretical[84] cross sections for electronic excitation from the metastable $a^1\Pi_u$ excited state to the $B^3\Pi_g$, $a'\ ^1\Sigma_u^-$ and $w^1\Delta_u$ states. Elastic cross sections for the $a^1\Pi_u$ states is also shown.

3.3. N_2^* ionization cross section

Metastable N_2 states, having lower ionization thresholds than the ground state, may contribute significantly to the ionization processes in gas discharges, especially in the DC regime.[139]

Experimental determination of ionization cross section of metastables or, more precisely, the electron-impact production of N_2^+ ions, presumably, in the process

$$e + N_2(A\ ^3\Sigma_u^+) \rightarrow N_2^+(\text{all states}) + 2\,e \qquad (10)$$

was made by Freund, Wetzel, and Shul.[124] In their method, the gas was first ionized in a DC discharge, a beam of N_2^+ ions extracted and then neutralized in the reaction chamber. The beam of neutral molecules obtained in this way contains also metastables. Results of Freund *et al.* are shown in Fig. 29. The maximum of their integral ionization cross section is observed at a lower energy than for the neutral molecule, as expected because the threshold for the ionization of metastables is lower than for the ground state N_2. However, the maximum of the total ionization of metastables is lower than the total ionization cross section of N_2. According to the Born–Bethe binary-collisions model (BEB),

$$\sigma = \sum_n 4\pi a_0^2 \xi_n \left(\frac{R}{I_n}\right)^2 \frac{1}{t+u_n+1} \times \left[1 + \frac{1}{t} + \frac{\ln t}{2}\left(1 - \frac{1}{t^2}\right) - \frac{\ln t}{t+1}\right], \qquad (11)$$

which predicts satisfacorily well cross sections for quite different molecules,[140] the cross section increases with decreasing the ionization threshold I_n. In the above equation, $t = E/I_n$ is the normalized

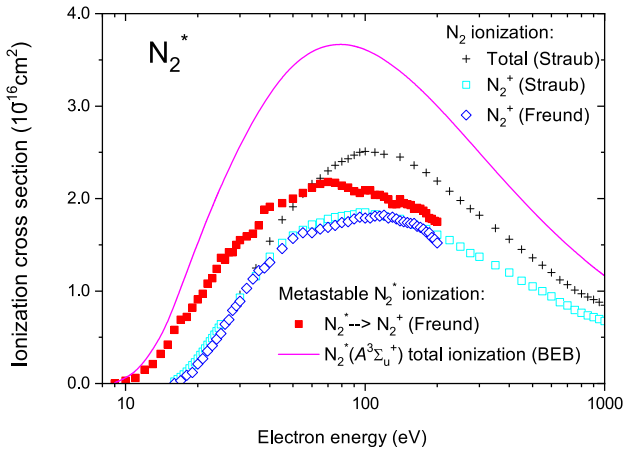

FIG. 29. Ionization cross section (N_2^+ yield) for the metastable N_2^* molecules: Red squares—the experiment by Freund, Wetzel, and Shul[124] and the solid curve—the BEB theory for the total ionization cross section of the N_2^* ($A\ ^3\Sigma^+$) state.[141] For comparison, the figure shows also Freund *et al.*'s cross sections for the N_2^+ production from N_2 with blue open diamonds, which agree with the recommended values by Straub *et al.*,[111] shown with cyan open squares.

electron impact energy, u_n is the normalized kinetic energy of molecular electrons (at a given orbital), ξ_n is the number of electrons at the nth orbital, a_0 is Bohr's radius, and R is the Rydberg constant. The BEB model was applied to N_2 in the $A^3\Sigma^+$ state by Laricchiuta, Celiberto, and Colonna;[141] the results are shown in Fig. 29.

The difference between the BEB fit[141] and the Freund, Wetzel, and Shul[124] experiment may be due to, at least, two reasons. The number of metastable molecules in the beam depends strongly on experimental conditions. In the measurements of Freund *et al.*, the metastable N_2 molecules—probably, only the long-lived $A^3\Sigma^+$ state—are formed in a collisional electron transfer between the N_2^+ beam, containing a significant fraction of the metastable ions N_2^+ in the $A^2\Pi_u$ state and triethylamine molecules. The cross section for the ionization of metastable N_2 was deduced from the signal of ions produced by electrons colliding at energies below the ionization threshold of the ground state of N_2. The complex dynamics of electron interacting with N_2 molecules in electronically excited states (see the earlier discussion) make it plausible that also other metastables, other than $A^3\Sigma^+$, like a or a', with higher ionization thresholds are present in the N_2 beam. This would lower the experimental cross section. Note that in their earlier paper, Armentrout *et al.*[142] used charge transfer with the NO molecule and obtained ionization cross section 50% lower at 100 eV than the more recent result.[124]

The second source of discrepancy may come from the BEB approach, which gives the total ionization cross section, while Freund *et al.*[124] detected only N_2^+ ions. Therefore, for the total ionization cross section of the $N_2^*(A^3\Sigma^+)$ molecule, we recommend the BEB results by Laricchiuta, Celiberto, and Colonna,[141] which are also supported by more accurate theoretical studies, such as using pure *ab initio* formalisms.

4. Molecular N_2^+ Ion

As discussed in Sec. 2.8, at 100 eV, more than a half of N_2^+ ions are created in the electronically excited states $A\ ^2\Pi_u$ and $B\ ^2\Sigma_u^+$. The optical emission from the B state of N_2^+ was observed in atmospheric-pressure microwave torches down to tens of centimeters from the discharge region.[13] N_2^+ is the most abundant ion in the F region (250 km altitude) of the Earth's ionosphere.[143] Recombination of N_2^+ ions with free electrons is the source of energetic N atoms, responsible of numerous processes in Earth's atmosphere,[144] including polar glows.

4.1. Dissociative recombination cross section

The dissociative recombination (DR) leads to formation of N atoms, while the cross section depends significantly on the initial vibrational state of the N_2^+ ion,

$$N_2^+(v^+) + e \rightarrow N + N. \quad (12)$$

The atoms are produced with few-eV kinetic energies. Four channels are exothermic,[18]

$$N_2^+ + e \rightarrow N(^4S) + N(^4S) + 5.82\ \text{eV}, \quad (13)$$

$$\rightarrow N(^2D) + N(^4S) + 3.44\ \text{eV}, \quad (14)$$

$$\rightarrow N(^2P) + N(^4S) + 2.24\ \text{eV}, \quad (15)$$

$$\rightarrow N(^2D) + N(^2D) + 1.05\ \text{eV}. \quad (16)$$

Branching ratios recommended by Dutuit *et al.*[18] are 0.25, 0.7, and 0.05, for ^4S, ^2D, and ^2P yields, respectively.

Sheehan and St.-Maurice[145] reviewing experimental studies noted that vibrationally excited ions yielded a lower recombination rate than the ground state. Little *et al.*[146] suggested that the DR rate from $N_2^+(v = 1)$ is significantly lower than for other vibrational states. It is difficult to cool N_2^+ because it has no dipole moment, allowing fast cooling of excited vibrational levels. Therefore, the vibrational distribution of N_2^+ and v^+-dependent DR cross sections should be accounted for in interpretations of experimental results and observations. For this reason, storage ring experiments were performed not only with symmetric isotopologue $^{14}N_2^+$ but also with $^{15}N^{14}N^+$, which has a small dipole moment (but still cools slowly).

Experiments in storage rings[147] and in merged beams,[145,148,149] as well as theoretical studies,[146,150] show, roughly, an $1/E$ dependence of the recombination cross section, with the value of about 4×10^{-14} cm^2 at 0.01 eV collisional energy. The calculations by Little *et al.*[146] agree well with the measurements if the vibrational distribution N_2^+ ions is accounted for, matching the one in the merged beams. The resulting rate coefficient[146] for the $v^+ = 0$ state is $2.568 \times 10^{-7}\ (T_e/300)^{-0.5166}$ for temperatures 300–800 K. The DR cross sections show resonances produced by Rydberg states of the ion attached to higher vibrational states of N_2^+, in the sub-eV region (see Fig. 30). The resonances were observed also in experiments.[148] The recent calculation by Abdoulanziz *et al.*[151] confirms earlier predictions[146,152] of a lower DR rate for the $v^+ = 1$ initial state of N_2^+ as compared to the $v^+ = 0$ state.

Recently, Abdoulanziz *et al.*[151] extended the calculation by Little *et al.*[146] to higher vibrational states of N_2^+ and electron temperatures 5000 K.

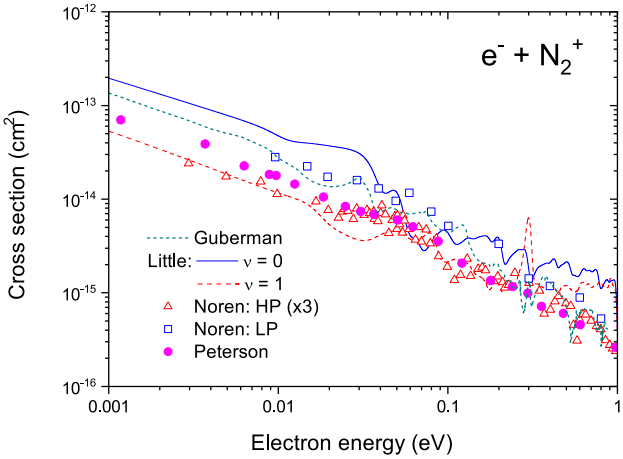

FIG. 30. Comparison of experimental and theoretical cross sections for DR: Theory is by Guberman[150] and Little *et al.*[146] and storage ring experiments are by Peterson *et al.*[147] Merged beam experiments are by Noren, Yousif, and Mitchell[148] whose results obtained at a low pressure agree with the merged beam experiments of Mul and McGowan[149] and with the swarm measurements of Mehr and Biondi,[153] while the results at a high pressure (and with a low extraction electrical field) are by few folds lower (here, we have multiplied them by a factor of 3; see the discussion in the text on the dependence of the dissociation on the initial vibrational state of the ion).

4.2. Vibrational excitation cross section

Vibrational excitations (and de-excitations) of the N_2^+ ion by an electron impact have recently been studied by Abdoulanziz *et al.*[151] for energies up to 2.3 eV. Cross sections for these processes show dense resonance structures produced by vibrational Rydberg resonances associated with closed vibrational levels of the ion, similar to those predicted for the DR. Inelastic transitions from six lowest $v_i^+ = 0 - 5$ vibrational levels to ten final levels $v_f^+ = 0 - 9$ were considered. The thermal rate coefficients were derived from the cross sections and fit to the analytical formula

$$k(T) = AT^{\alpha} \exp\left(-\frac{B}{T}\right) \tag{17}$$

with three parameters A, B, and α for each transition. We recommend to use the thermal rate coefficients for those transitions. The parameters for transitions starting from the ground vibrational level to $v_f^+ = 1 - 9$ are reproduced in Table 11. The rate coefficients for these transitions are also shown in Fig. 31. Parameters for transitions starting from excited vibrational levels $v_i^+ = 1 - 5$ can be found in Table III of the study by Abdoulanziz *et al.*[151]

The rate coefficients for $v_i^+ = 0 \rightarrow v_f^+ = 0, \ldots, 9$ are also shown in Fig. 31.

4.3. N_2^+ ionization cross section

According to recent calculations,[146,150,154] the DR cross section drops to few Å^2 at 1 eV. At higher energies, other inelastic processes, such as the electron-impact dissociation and ionization,

$$N_2^+ + e \rightarrow N + N^+ + e \quad \text{(dissociation)}, \tag{18}$$

$$N_2^+ + e \rightarrow N_2^+ + 2e \quad \text{(ionization)}, \tag{19}$$

$$N_2^+ + e \rightarrow N^+ + N^+ + 2e \quad \text{(dissociative ionization)}, \tag{20}$$

have also significant cross sections.

Experimental thresholds[155] for these processes are 8.4, 27.9, and 31.2 eV, respectively. These values agree with thresholds for similar processes of ionization of the N_2 molecule (adding 15.8 eV for the formation of the N_2^+ ion from N_2).

There are few experiments on the ionization and/or dissociation of N_2^+. Peterson *et al.*[147] determined the cross section for the sum of processes (19) and (20) (along with the DR) in a storage ring experiment. Bahati *et al.*[155] used a table-top crossed-beam experiment. They separated signals from single processes Eqs. (18)–(20) by a magnetic-deflection sweeping of the ions formed over the aperture of the detector. As the processes of Eqs. (18)–(20) differ by the spread in kinetic energies of the ions formed, a careful deconvolution procedure allows them to separate the single reaction channels. The cross sections derived in this way are shown in Fig. 32.

To obtain the total ionization cross section, Bahati *et al.*[155] added the (single) ionization cross section of Eq. (19) and the double of the dissociative ionization cross section of Eq. (20). Even if the

TABLE 11. Parameters for recommended rate coefficients for vibrational excitation of the N_2^+ ion from the ground vibrational level $v_i^+ = 0$ to the nine lowest levels $v_f^+ = 1, \ldots, 9$

v_f^+	A	α	B
1	3.355×10^{-6}	−0.584	4 525.43
2	9.137×10^{-7}	−0.554	6 100.88
3	4.984×10^{-6}	−0.699	9 626.89
4	9.306×10^{-8}	−0.292	11 989.3
5	8.925×10^{-7}	−0.596	14 871.8
6	1.447×10^{-6}	−0.668	17 980.5
7	1.656×10^{-6}	−0.696	21 345
8	9.867×10^{-8}	−0.471	23 504.3
9	1.340×10^{-6}	−0.780	26 309.7

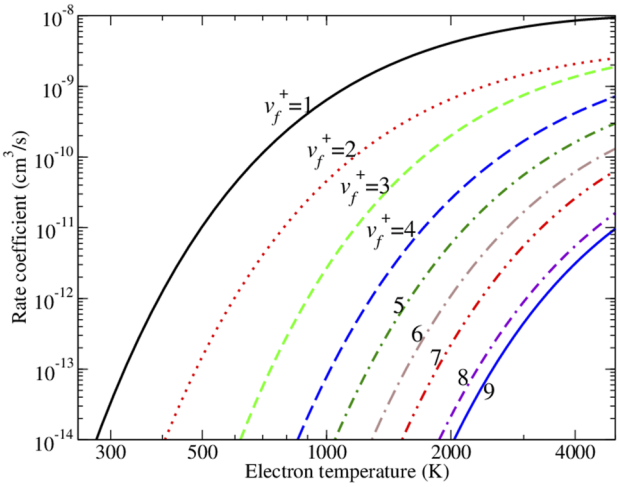

FIG. 31. Thermal rate coefficients for vibrational excitation of N_2^+ from $v_i^+ = 0$ to $v_f^+ = 0, \ldots, 9$.[151]

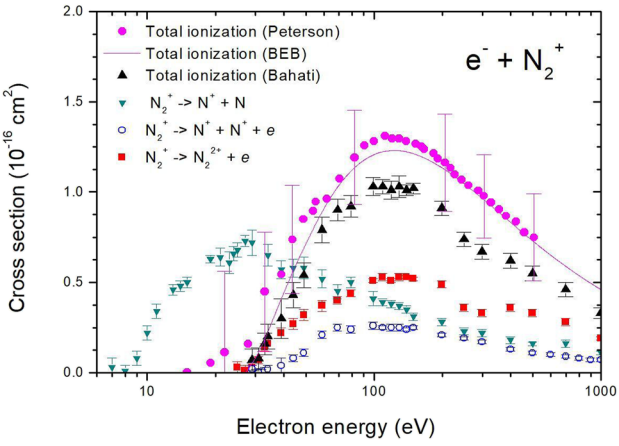

FIG. 32. ICSs for the dissociation of the N_2^+ ion: Eq. (18)—small down triangles, ionization Eq. (19)—red full squares, and dissociative ionization, Eq. (20) as measured in crossed-beams experiment by Bahati *et al.*[155]—open circles. Up black triangles is the sum of the two ionization channels as reported by Bahati *et al.*[155] The data by Peterson *et al.*[147]—full (magenta) circles—have been digitalized from a figure by Bahati *et al.*[155]

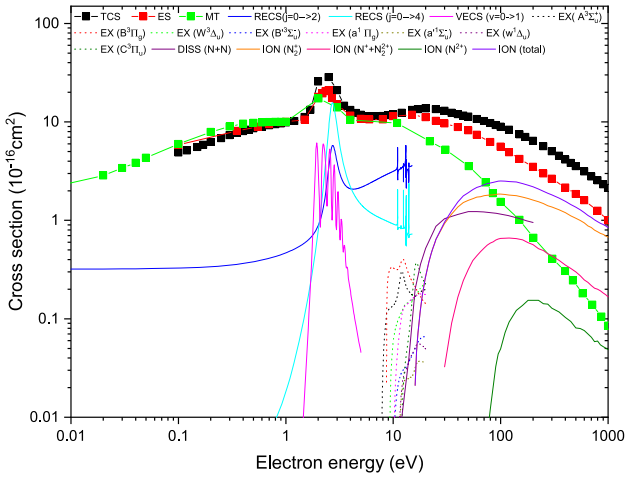

FIG. 33. Summary of recommended cross section for electron collisions with N_2. TCS—total scattering, ES—elastic scattering, MT—momentum transfer, ION—ionization, VECS—vibrational excitation, RECS—rotational excitation, EX—electronic excitation, and DISS—neutral dissociation.

reported[155] uncertainties seem to be underestimated, the two experimental determinations[147,155] of the total N_2^+ ionization cross section seem to be consistent (see Fig. 32). They agree also with the BEB calculation (with restricted Hartree–Fock orbitals) by Kim, Irikura, and Ali.[156] We use the BEB calculation as the recommended values for the total ionization cross section of N_2^+, while for the single channels [Eq. (18)–(20)], we recommend the results by Bahati *et al.*[155] with ±20% uncertainty.

5. Summary and Future work

This paper reviews available cross sections resulting from electron collisions with molecular nitrogen with aim of compiling a complete dataset of cross sections for plasma and other studies. Compared to other electron–molecule collision cross sections that we have reviewed,[157] there are relatively complete, accurate, and consistent sets of data available for electron–N_2 collisions. Figure 33 summarizes our recommended electron collision cross sections. The main low-energy cross section for which experimental information is largely missing is electron impact rotational excitation, which, in any case, is expected to have small cross sections, which should be amenable to calculation. Nitrogen plasmas show characteristic emission for long-lived electronically excited states. The first predictions of electron collision cross sections with such states have recently become available, but clearly these should be tested in models and improved on. Finally, we consider electron collision processes with N_2^+; recent calculations have given extensive datasets on DR and vibrational excitation cross sections, which appear to be in agreement with the more limited experimental studies for this collision system.

6. Supplementary material

Corresponding numerical data according to figure numbers are included in the supplementary material.

7. Acknowledgments

We thank Nigel Mason for helpful discussions. This research was partially supported by the R&D Program Plasma Big Data ICT Convergence Technology Research Project through the Korea Institute of Fusion Energy (KFE) funded by the Ministry of Science and Technology Information and Communication, Republic of Korea. It was also partially supported by the Technology Innovation Program (Code No. 1415178875, Development and Dissemination on National Standard Reference Data) funded by the Ministry of Trade, Industry and Energy (MOTIE, Republic of Korea) and the U.S. National Science Foundation (Grants Nos. 2110279 and 2102188).

8. Author Declarations

8.1. Conflict of interest

The authors have no conflicts to disclose.

9. Data Availability

The data that support the findings of this study are available within the article and its supplementary material and from the corresponding author upon reasonable request.

10. References

[1]V. A. Krasnopolsky, "Chemical composition of Titan's atmosphere and ionosphere: Observations and the photochemical model," Icarus **236**, 83–91 (2014).
[2]J. L. Elliot, D. F. Strobel, X. Zhu, J. A. Stansberry, L. H. Wasserman, and O. G. Franz, "The thermal structure of Triton's middle atmosphere," Icarus **143**, 425–428 (2000).
[3]V. A. Krasnopolsky, "A photochemical model of Pluto's atmosphere and ionosphere," Icarus **335**, 113374 (2020).
[4]P. B. Rimmer and S. Rugheimer, "Hydrogen cyanide in nitrogen-rich atmospheres of rocky exoplanets," Icarus **329**, 124–131 (2019).
[5]A. Tsiaras, I. P. Waldmann, G. Tinetti, J. Tennyson, and S. N. Yurchenko, "Water vapour in the atmosphere of the habitable-zone eight-Earth-mass planet K2-18b," Nat. Astron. **3**, 1086–1091 (2019).
[6]R. A. Armstrong, D. M. Suszcynsky, W. A. Lyons, and T. E. Nelson, "Multi-color photometric measurements of ionization and energies in sprites," Geophys. Res. Lett. **27**, 653–656, https://doi.org/10.1029/1999gl003672 (2000).
[7]V. Guerra, P. A. Sá, and J. Loureiro, "Nitrogen pink afterglow: The mystery continues," J. Phys.: Conf. Ser. **63**, 012007 (2007).
[8]B. Gordiets and A. Ricard, "Production of N, O and NO in N_2-O_2 flowing discharges," Plasma Sources Sci. Technol. **2**, 158–163 (1993).
[9]Z. Li, T. Ozawa, I. Sohn, and D. A. Levin, "Modeling of electronic excitation and radiation in non-continuum hypersonic reentry flows," Phys. Fluids **23**, 066102 (2011).
[10]J. Annaloro and A. Bultel, "Vibrational and electronic collisional-radiative model in air for Earth entry problems," Phys. Plasmas **21**, 123512 (2014).
[11]I. N. Kadochnikov, B. I. Loukhovitski, and A. M. Starik, "Thermally nonequilibrium effects in shock-induced nitrogen plasma: Modelling study," Plasma Sources Sci. Technol. **22**, 035013 (2013).
[12]Z. Lianzhu, Z. Shuxia, and M. Xiulan, "Characterization of nitrogen glow discharge plasma via optical emission spectrum simulation," Plasma Sci. Technol. **10**, 455–462 (2008).
[13]C.-J. Chen and S.-Z. Li, "Investigation of a nitrogen post-discharge of an atmospheric-pressure microwave plasma torch by optical emission spectroscopy," Phys. Plasmas **24**, 033512 (2017).
[14]J. M. Ajello, J. S. Evans, V. Veibell, C. P. Malone, G. M. Holsclaw, A. C. Hoskins, R. A. Lee, W. E. McClintock, S. Aryal, R. W. Eastes, and N. Schneider, "The UV

spectrum of the Lyman-Birge-Hopfield band system of N_2 induced by cascading from electron impact," J. Geophys. Res.: Space Phys. **125**, e2019JA027546, https://doi.org/10.1029/2019ja027546 (2020).
[15] A. M. Gatey, S. S. Hosmani, S. B. Arya, C. A. Figueroa, and R. P. Singh, "Plasma nitriding of AISI 2205 steel: Effects of surface mechanical attrition treatment and chemical etching," Surf. Eng. **32**, 61–68 (2016).
[16] M. Oberkofler, D. Douai, S. Brezinsek, J. W. Coenen, T. Dittmar, A. Drenik, S. G. Romanelli, E. Joffrin, K. McCormick, M. Brix, G. Calabro, M. Clever, C. Giroud, U. Kruezi, K. Lawson, C. Linsmeier, A. M. Rojo, A. Meigs, S. Marsen, R. Neu, M. Reinelt, B. Sieglin, G. Sips, M. Stamp, and F. L. Tabares, "First nitrogen-seeding experiments in JET with the ITER-like Wall," J. Nucl. Mater. **438**, S258–S261 (2013).
[17] C. Pattyn, N. Maira, A. Remy, N. C. Roy, S. Iseni, D. Petitjean, and F. Reniers, "Potential of N_2/O_2 atmospheric pressure needle-water DC microplasmas for nitrogen fixation: Nitrite-free synthesis of nitrates," Phys. Chem. Chem. Phys. **22**, 24801–24812 (2020).
[18] O. Dutuit, N. Carrasco, R. Thissen, V. Vuitton, C. Alcaraz, P. Pernot, N. Balucani, P. Casavecchia, A. Canosa, S. Le Picard, J.-C. Loison, Z. Herman, J. Zabka, D. Ascenzi, P. Tosi, P. Franceschi, S. D. Price, and P. Lavvas, "Critical review of N, N^+, N_2^+, N^{++}, and N_2^{++} main production processes and reactions of relevance to Titan's atmosphere," Astrophys. J., Suppl. Ser. **204**, 20 (2013).
[19] A. Bultel and J. Annaloro, "Elaboration of collisional–radiative models for flows related to planetary entries into the Earth and Mars atmospheres," Plasma Sources Sci. Technol. **22**, 025008 (2013).
[20] M. Capitelli, G. Colonna, G. D'Ammando, V. Laporta, and A. Laricchiuta, "Nonequilibrium dissociation mechanisms in low temperature nitrogen and carbon monoxide plasmas," Chem. Phys. **438**, 31–36 (2014).
[21] M. Capitelli, R. Celiberto, G. Colonna, F. Esposito, C. Gorse, K. Hassouni, A. Laricchiuta, and S. Longo, "Self-consistent kinetics of molecular plasmas: The nitrogen case," in *Fundamental Aspects of Plasma Chemical Physics: Kinetics*, *Springer Series on Atomic Optical and Plasma Physics Vol. 85* (Springer, New York, 2016), pp. 223–245.
[22] E. Vervloessem, M. Aghaei, F. Jardali, N. Hafezkhiabani, and A. Bogaerts, "Plasma-based N_2 fixation into NO_x: Insights from modeling toward optimum yields and energy costs in a gliding arc plasmatron," ACS Sustainable Chem. Eng. **8**, 9711–9720 (2020).
[23] F. Jardali, S. Van Alphen, J. Creel, H. Ahmadi Eshtehardi, M. Axelsson, R. Ingels, R. Snyders, and A. Bogaerts, "NO_x production in a rotating gliding arc plasma: Potential avenue for sustainable nitrogen fixation," Green Chem. **23**, 1748–1757 (2021).
[24] S. Van Alphen, F. Jardali, J. Creel, G. Trenchev, R. Snyders, and A. Bogaerts, "Sustainable gas conversion by gliding arc plasmas: A new modelling approach for reactor design improvement," Sustainable Energy Fuels **5**, 1786–1800 (2021).
[25] J. Tennyson, S. Mohr, M. Hanicinec, A. Dzarasova, C. Smith, S. Waddington, B. Liu, L. L. Alves, K. Bartschat, A. Bogaerts, S. U. Engelmann, T. Gans, A. R. Gibson, S. Hamaguchi, K. R. Hamilton, C. Hill, D. O'Connell, S. Rauf, K. van 't Veer, and O. Zatsarinny, "The 2021 release of the Quantemol database (QDB) of plasma chemistries and reactions," Plasma Sources Sci. Technol. **31**, 095020 (2022).
[26] Y. Itikawa, "Cross sections for electron collisions with nitrogen molecules," J. Phys. Chem. Ref. Data **35**, 31–53 (2006).
[27] T. Tabata, T. Shirai, M. Sataka, and H. Kubo, "Analytic cross sections for electron impact collisions with nitrogen molecules," At. Data Nucl. Data Tables **92**, 375–406 (2006).
[28] S. Kawaguchi, K. Takahashi, and K. Satoh, "Electron collision cross section set for N_2 and electron transport in N_2, N_2/He, and N_2/Ar," Plasma Sources Sci. Technol. **30**, 035010 (2021).
[29] G. J. Schulz, "Vibrational excitation of N_2, CO, and H_2 by electron impact," Phys. Rev. **135**, A988 (1964).
[30] R. E. Kennerly, "Absolute total electron scattering cross sections for N_2 between 0.5 and 50 eV," Phys. Rev. A **21**, 1876 (1980).
[31] G. P. Karwasz, R. S. Brusa, and D. Pliszka, "Energy scale determination and energy resolution in positron total cross section measurements," J. Phys.: Conf. Ser. **199**, 012019 (2010).
[32] M.-Y. Song, J.-S. Yoon, H. Cho, Y. Itikawa, G. P. Karwasz, V. Kokoouline, Y. Nakamura, and J. Tennyson, "Cross sections for electron collisions with methane," J. Phys. Chem. Ref. Data **44**, 023101 (2015).
[33] C. Szmytkowski, K. Maciag, and G. Karwasz, "Absolute electron-scattering total cross section measurements for noble gas atoms and diatomic molecules," Phys. Scr. **54**, 271 (1996).
[34] G. Karwasz, R. Brusa, and A. Zecca, "6.1 total scattering cross section: Datasheet from Landolt-Börnstein—Group I elementary particles, nuclei and atoms," in *Interactions of Photons and Electrons with Molecules*, *Springer Materials Vol. 17C* (Springer-Verlag, Berlin, Heidelberg, 2003).
[35] C. Szmytkowski and P. Możejko, "Recent total cross section measurements in electron scattering from molecules," Eur. Phys. J. D **74**, 90 (2020).
[36] K. R. Hoffman, M. S. Dababneh, Y.-F. Hsieh, W. E. Kauppila, V. Pol, J. H. Smart, and T. S. Stein, "Total-cross-section measurements for positrons and electrons colliding with H_2, N_2, and CO_2," Phys. Rev. A **25**, 1393 (1982).
[37] O. Sueoka and S. Mori, "Total cross sections for positrons and electrons colliding with N_2, CO and CO_2 molecules," J. Phys. Soc. Jpn. **53**, 2491 (1984).
[38] M. Kitajima, T. Kishino, T. Okumura, N. Kobayashi, A. Sayama, Y. Mori, K. Hosaka, T. Odagiri, M. Hoshino, and H. Tanaka, "Low-energy and very-low energy total cross sections for electron collisions with N_2," Eur. Phys. J. D **71**, 139 (2017).
[39] W. Sun, M. A. Morrison, W. A. Isaacs, W. K. Trail, D. T. Alle, R. J. Gulley, M. J. Brennan, and S. J. Buckman, "Detailed theoretical and experimental analysis of low-energy electron-N_2 scattering," Phys. Rev. A **52**, 1229–1256 (1995).
[40] J. Ferch, W. Raith, and A. Schweiker, "Total electron scattering cross sections for N2 at low electron energies," in *Abstracts XVII International Conference on Physics of Electronic and Atomic Collisions (Brisbane)* edited by I. E. McCarthy, M. C. Standage, and W. R. MacGillivray (A. Hilger, Bristol, 1991), p. 211.
[41] A. I. Lozano, J. C. Oller, K. Krupa, F. Ferreira da Silva, P. Limão-Vieira, F. Blanco, A. Muñoz, R. Colmenares, and G. García, "Magnetically confined electron beam system for high resolution electron transmission-beam experiments," Rev. Sci. Instrum. **89**, 063105 (2018).
[42] K. Jost, P. G. F. Bisling, F. Eschen, M. Felsmann, and L. Walther, "Total-cross-section measurements for electron scattering from N_2, Xe, Kr and Ar," in *Abstracts XIII International Conference on Physics of Electronic and Atomic Collisions (Berlin),* edited by J. Eichler, W. Fritsch, I.V. Hertel, N. Stolterfoht, and U. Wille (North Holland, Berlin, 1983), p. 91.
[43] S. V. Hoffmann, S. L. Lunt, N. C. Jones, D. Field, and J.-P. Ziesel, "An undulator-based spherical grating monochromator beamline for low energy electron-molecule scattering experiments," Rev. Sci. Instrum. **73**, 4157–4163 (2002).
[44] T. Okumura, N. Kobayashi, A. Sayama, Y. Mori, H. Akasaka, K. Hosaka, T. Odagiri, M. Hoshino, and M. Kitajima, "Total cross-section for low-energy and very low-energy electron collisions with O_2," J. Phys. B: At., Mol. Opt. Phys. **52**, 035201 (2019).
[45] M. Allan, "Excitation of vibrational levels up to $v = 17$ in N_2 by electron impact in the 0-5 eV region," J. Phys. B: At., Mol. Opt. Phys. **18**, 4511 (1985).
[46] J. C. Nickel, I. Kanik, S. Trajmar, and K. Imre, "Total cross section measurements for electron scattering on H_2 and N_2 from 4 to 300 eV," J. Phys. B: At., Mol. Opt. Phys. **25**, 2427 (1992).
[47] T. H. Hoffman, M. Allan, K. Franz, M.-W. Ruf, H. Hotop, G. Sauter, and W. Meyer, "Resonance structure in electron–N_2 scattering around 11.5 eV: High-resolution measurements, *ab initio* calculations and line shape analyses," J. Phys. B: At., Mol. Opt. Phys. **42**, 215202 (2009).
[48] Z. Idziaszek and G. Karwasz, "Modified effective-range theory for low energy e-N_2 scattering," Eur. Phys. J. D **51**, 347–355 (2009).
[49] G. Karwasz, R. S. Brusa, A. Gasparoli, and A. Zecca, "Total cross-section measurements for e^- —CO scattering: 80–4000 eV," Chem. Phys. Lett. **211**, 529–533 (1993).
[50] G. García, A. Pérez, and J. Campos, "Total cross section for electron scattering from N_2 in the energy range 600–5000 eV," Phys. Rev. A **38**, 654 (1988).
[51] M.-Y. Song, J.-S. Yoon, H. Cho, G. P. Karwasz, V. Kokoouline, Y. Nakamura, and J. Tennyson, "Electron collision cross sections with NO, N_2O and NO_2," J. Phys. Chem. Ref. Data **48**, 043104 (2019).
[52] A. Zecca, J. C. Nogueira, G. P. Karwasz, and R. S. Brusa, "Total cross sections for electron scattering on NO_2, OCS, SO_2 at intermediate energies," J. Phys. B: At., Mol. Opt. Phys. **28**, 477 (1995).

[53]S. K. Srivastava, A. Chutjian, and S. Trajmar, "Absolute elastic differential electron scattering cross sections in the intermediate energy region. II.—N_2," J. Chem. Phys. **64**, 1340–1344 (1976).
[54]T. W. Shyn and G. R. Carignan, "Angular distribution of electrons elastically scattered from gases: 1.5-400 eV on N_2. II," Phys. Rev. A **22**, 923–929 (1980).
[55]W. Sohn, K.-H. Kochem, K.-M. Scheuerlein, K. Jung, and H. Ehrhardt, "Near-threshold vibrational excitation and elastic electron scattering from N_2," J. Phys. B: At., Mol. Opt. Phys. **19**(23), 4017 (1986).
[56]J. C. Nickel, C. Mott, I. Kanik, and D. C. McCollum, "Absolute elastic differential electron scattering cross sections for carbon monoxide and molecular nitrogen in the intermediate energy region," J. Phys. B: At., Mol. Opt. Phys. **21**, 1867 (1988).
[57]M. J. Brennan, D. T. Alle, P. Euripides, S. J. Buckman, and M. J. Brunger, "Elastic electron scattering and rovibrational excitation of N_2 at low incident energies," J. Phys. B: At., Mol. Opt. Phys. **25**(11), 2669 (1992).
[58]X. Shi, T. M. Stephen, and P. D. Burrow, "Differential cross sections for elastic scattering of electrons from N_2 at 0.55, 1.5 and 2.2 eV," J. Phys. B: At., Mol. Opt. Phys. **26**, 121 (1993).
[59]M. Zubek, B. Mielewska, and G. C. King, "Absolute differential cross sections for electron elastic scattering and vibrational excitation in nitrogen in the angular range from 120 to 180," J. Phys. B: At., Mol. Opt. Phys. **33**, L527 (2000).
[60]M. Allan, "Measurement of the elastic and $v = 0 \rightarrow 1$ differential electron–N_2 cross sections over a wide angular range," J. Phys. B: At., Mol. Opt. Phys. **38**, 3655–3672 (2005).
[61]J. Muse, H. Silva, M. C. A. Lopes, and M. A. Khakoo, "Low energy elastic scattering of electrons from H_2 and N_2," J. Phys. B: At., Mol. Opt. Phys. **41**, 095203 (2008).
[62]I. Linert and M. Zubek, "Differential cross sections for electron elastic scattering and vibrational $v = 1$ excitation in nitrogen in the energy range from 5 to 20 eV measured over an angular range of 100°-180°," J. Phys. B: At., Mol. Opt. Phys. **42**, 085203 (2009).
[63]S. J. Buckman, M. Brunger, and M. T. Elford, "6.2 integral elastic cross sections: Datasheet from Landolt-Börnstein—Group I elementary particles, nuclei and atoms," in *Interactions of Photons and Electrons with Molecules*, *Springer Materials Vol. 17C* (Springer-Verlag, Berlin, Heidelberg, 2003).
[64]R. D. DuBois and M. E. Rudd, "Differential cross sections for elastic scattering of electrons from argon, neon, nitrogen and carbon monoxide," J. Phys. B: At., Mol. Opt. Phys. **9**, 2657–2667 (1976).
[65]M. T. Elford, S. J. Buckman, and M. Brunger, "6.3 elastic momentum transfer cross sections: Datasheet from Landolt-Börnstein—Group I elementary particles, nuclei and atoms," in *Interactions of Photons and Electrons with Molecules*, *Springer Materials Vol. 17C* (Springer-Verlag, Berlin, Heidelberg, 2003).
[66]G. Haddad, "Cross sections for electron scattering in nitrogen," Aust. J. Phys. **37**, 487–494 (1984).
[67]L. Landau and E. Lifshitz, *Quantum Mechanics: Non-Relativistic Theory* (Butterworth Heinemann, Burlington, MA, 2003).
[68]Y. Itikawa and N. Mason, "Rotational excitation of molecules by electron collisions," Phys. Rep. **414**, 1–41 (2005).
[69]H. Kutz and H.-D. Meyer, "Rotational excitation of N_2 and Cl_2 molecules by electron impact in the energy range 0.01–1000 eV: Investigation of excitation mechanisms," Phys. Rev. A **51**, 3819 (1995).
[70]M. A. Morrison, W. Sun, W. A. Isaacs, and W. K. Trail, "Ultrasimple calculation of very-low-energy momentum-transfer and rotational-excitation cross sections: e-N_2 scattering," Phys. Rev. A **55**, 2786 (1997).
[71]S. Telega, E. Bodo, and F. A. Gianturco, "Rotationally inelastic collisions of electrons with H_2 and N_2 molecules: Converged space-frame calculations at low energies," Eur. Phys. J. D **29**, 357–365 (2004).
[72]M. Šulc, R. Čurík, J.-P. Ziesel, N. C. Jones, and D. Field, "A new type of interference phenomenon in cold collisions of electrons with N_2," J. Phys. B: At., Mol. Opt. Phys. **44**, 195204 (2011).
[73]L. L. Alves, "The IST-LISBON database on LXCat," J. Phys.: Conf. Ser. **565**, 012007 (2014).
[74]Z. Mašín, J. Benda, J. D. Gorfinkiel, A. G. Harvey, and J. Tennyson, "UKRmol+: A suite for modelling electronic processes in molecules interacting with electrons, positrons and photons using the R-matrix method," Comput. Phys. Commun. **249**, 107092 (2020).
[75]B. Cooper, M. Tudorovskaya, S. Mohr, A. O'Hare, M. Hanicinec, A. Dzarasova, J. Gorfinkiel, J. Benda, Z. Mašín, A. Al-Refaie, P. J. Knowles, and J. Tennyson, "Quantemol electron collisions (QEC): An enhanced expert system for performing electron molecule collision calculations using the R-matrix method," Atoms **7**, 97 (2019).
[76]H. Tanaka, T. Yamamoto, and T. Okada, "Electron impact cross sections for $v = 0 \rightarrow 1$ vibrational excitation of N_2 at electron energies from 3 to 30 eV," J. Phys. B: At., Mol. Opt. Phys. **14**(12), 2081 (1981).
[77]V. Laporta, D. A. Little, R. Celiberto, and J. Tennyson, "Electron-impact resonant vibrational excitation and dissociation processes involving vibrationally excited N_2 molecules," Plasma Sources Sci. Technol. **23**, 065002 (2014).
[78]M. Vicic, G. Poparic, and D. S. Belic, "Large vibrational excitation of by low-energy electrons," J. Phys. B: At., Mol. Opt. Phys. **29**, 1273 (1996).
[79]Y. Ohmori, M. Shimozuma, and H. Tagashira, "Boltzmann equation analysis of electron swarm behaviour in nitrogen," J. Phys. D: Appl. Phys. **21**, 724–729 (1988).
[80]A. V. Phelps and L. C. Pitchford, "Anisotropic scattering of electrons by N_2 and its effect on electron transport," Phys. Rev. A **31**, 2932–2949 (1985).
[81]C. J. Gillan, J. Tennyson, B. M. McLaughlin, and P. G. Burke, "Low-energy electron impact excitation of the nitrogen molecule: Optically forbidden transitions," J. Phys. B: At., Mol. Opt. Phys. **29**, 1531–1547 (1996).
[82]M. Tashiro and K. Morokuma, "*R*-matrix calculation of integral and differential cross sections for low-energy electron-impact excitations of the N_2 molecule," Phys. Rev. A **75**, 012720 (2007).
[83]R. F. Da Costa and M. A. P. Lima, "Excitation of the $a^1\Pi_g$ and $B^3\Pi_g$ electronic states of the nitrogen molecule by electron impact," Int. J. Quantum Chem. **106**, 2664–2676 (2006).
[84]H. Su, X. Cheng, H. Zhang, and J. Tennyson, "Electron collisions with molecular nitrogen in its ground and electronically excited states using the R-matrix method," J. Phys. B: At., Mol. Opt. Phys. **54**, 115203 (2021).
[85]H. Su, X. Cheng, B. Cooper, J. Tennyson, and H. Zhang, "Electron-impact high-lying N_2^- resonant states," Phys. Rev. A **105**, 062824 (2022).
[86]J. Oddershede, N. E. Grüner, and G. H. F. Diercksen, "Comparison between equation of motion and polarization propagator calculations," Chem. Phys. **97**, 303–310 (1985).
[87]M. A. Khakoo, P. V. Johnson, I. Ozkay, P. Yan, S. Trajmar, and I. Kanik, "Differential cross sections for the electron impact excitation of the $A^3\Sigma_u^+$, $B^3\Pi_g$, $W^3\Delta_u$, $B'^3\Sigma_u^-$, $a'^1\Sigma_u^-$, $a^1\Pi_g$, $w^1\Delta_u$, and $C^3\Pi_u$ states of N_2," Phys. Rev. A **71**, 062703 (2005).
[88]P. V. Johnson, C. P. Malone, I. Kanik, K. Tran, and M. A. Khakoo, "Integral cross sections for the direct excitation of the $A\ ^3\Sigma_u^+$, $B\ ^3\Pi_g$, $W\ ^3\Delta_u$, $B'\ ^3\Sigma_u^-$, $a'\ ^1\Sigma_u^-$, $a\ ^1\Pi_g$, $w\ ^1\Delta_u$, and $C\ ^3\Pi_u$ electronic states in N_2 by electron impact," J. Geophys. Res. **110**, A11311, https://doi.org/10.1029/2005ja011295 (2005).
[89]S. Trajmar, D. F. Register, and A. Chutjian, "Electron scattering by molecules II. Experimental methods and data," Phys. Rep. **97**, 219 (1983).
[90]C. P. Malone, P. V. Johnson, X. Liu, B. Ajdari, I. Kanik, and M. A. Khakoo, "Integral cross sections for the electron-impact excitation of the $b^1\Pi_u$, $c_3\ ^1\Pi_u$, $o_3\ ^1\Pi_u$, $b'\ ^1\Sigma_u^+$, $c'_4\ 1\Sigma_u+$, $G^3\Pi_u$, and $F^3\Pi_u$ states of N_2," Phys. Rev. A **85**, 062704 (2012).
[91]L. Campbell, M. J. Brunger, A. M. Nolan, L. J. Kelly, A. B. Wedding, J. Harrison, P. J. O. Teubner, D. C. Cartwright, and B. McLaughlin, "Integral cross sections for electron impact excitation of electronic states of N_2," J. Phys. B: At., Mol. Opt. Phys. **34**, 1185–1199 (2001).
[92]C. P. Malone, P. V. Johnson, J. A. Young, X. Liu, B. Ajdari, M. A. Khakoo, and I. Kanik, "Integral cross sections for electron-impact excitation of the $C^3\Pi_u$, $E^3\Sigma^+{}_g$ and $a''\ ^1\Sigma_g^+$ states of N_2," J. Phys. B: At., Mol. Opt. Phys. **42**, 225202 (2009).
[93]H. Tanaka, M. J. Brunger, L. Campbell, H. Kato, M. Hoshino, and A. R. P. Rau, "Scaled plane-wave Born cross sections for atoms and molecules," Rev. Mod. Phys. **88**, 025004 (2016).
[94]E. N. Lassettre, "Power series representation of generalized oscillator strengths," J. Chem. Phys. **43**, 4479–4486 (1965).
[95]Y.-G. Peng, X. Kang, K. Yang, X.-L. Zhao, Y.-W. Liu, X.-X. Mei, W.-Q. Xu, N. Hiraoka, K.-D. Tsuei, and L.-F. Zhu, "Squared form factors of vibronic excitations in 12–13.3 eV of nitrogen studied by high-resolution inelastic x-ray scattering," Phys. Rev. A **89**, 032512 (2014).

[96]Y. W. Liu, L. Q. Xu, D. D. Ni, X. Xu, X. C. Huang, and L. F. Zhu, "Integral cross sections of the dipole-allowed excitations of nitrogen molecule studied by the fast electron scattering," J. Geophys. Res.: Space Phys. **122**, 3459–3468, https://doi.org/10.1002/2016ja023857 (2017).
[97]H. J. Blaauw, R. W. Wagenaar, D. H. Barends, and F. J. de Heer, "Total cross sections for electron scattering from N_2 and He," J. Phys. B: Atom. Mol. Phys. **13**, 359 (1980).
[98]N. J. Mason and W. R. Newell, "Electron impact total excitation cross section of the $a^1\Pi_g$ state of N_2," J. Phys. B: At., Mol. Opt. Phys. **20**, 3913 (1987).
[99]M. Zubek, "Excitation of the $C^3\Pi_u$ state of N_2 by electron impact in the near-threshold region," J. Phys. B: At., Mol. Opt. Phys. **27**, 573 (1994).
[100]D. C. Frost and C. A. McDowell, "The dissociation energy of the nitrogen molecule," Proc. R. Soc. A **236**, 278–284 (1956).
[101]P. C. Cosby, "Electron-impact dissociation of nitrogen," J. Chem. Phys. **98**, 9544 (1993).
[102]J. Almlöf, B. J. Deleeuw, P. R. Taylor, C. W. Bauschlicher, Jr., and P. Siegbahn, "The dissociation energy of N_2," Int. J. Quantum Chem. **36**, 345–354 (1989).
[103]K. L. Heritier, R. L. Jaffe, V. Laporta, and M. Panesi, "Energy transfer models in nitrogen plasmas: Analysis of $N_2(X\,^1\Sigma_g^+)$–$N(^4S_u)$–e^- interaction," J. Chem. Phys. **141**, 184302 (2014).
[104]U. Bley, M. Koch, F. Temps, P. B. Davies, and I. H. Davis, "Measurement of the $^2D_{5/2}$–$^2D_{3/2}$ fine structure interval in metastable nitrogen atoms at 1.15 mm by laser magnetic resonance," J. Chem. Phys. **90**, 628–632 (1989).
[105]H. F. Winters, "Ionic adsorption and dissociation cross section for nitrogen," J. Chem. Phys. **44**, 1472–1476 (1966).
[106]D. Rapp and P. Englander-Golden, "Total cross sections for ionization and attachment in gases by electron impact. I. Positive ionization," J. Chem. Phys. **43**, 1464–1479 (1965).
[107]E. C. Zipf and R. W. McLaughlin, "On the dissociation of nitrogen by electron impact and by E.U.V. photo-absorption," Planet. Space Sci. **26**, 449–462 (1978).
[108]L. Mi and R. A. Bonham, "Electron–ion coincidence measurements: The neutral dissociation plus excitation cross section for N_2," J. Chem. Phys. **108**, 1904–1909 (1998).
[109]C. Tian and C. R. Vidal, "Electron impact ionization of N_2 and O_2: Contributions from different dissociation channels of multiply ionized molecules," J. Phys. B: At., Mol. Opt. Phys. **31**, 5369–5381 (1998).
[110]T. Majeed and D. J. Strickland, "New survey of electron impact cross sections for photoelectron and auroral electron energy loss calculations," J. Phys. Chem. Ref. Data **26**, 335–349 (1997).
[111]H. C. Straub, P. Renault, B. G. Lindsay, K. A. Smith, and R. F. Stebbings, "Absolute partial cross sections for electron-impact ionization of H_2, N_2, and O_2 from threshold to 1000 eV," Phys. Rev. A **54**, 2146–2153 (1996).
[112]B. L. Schram, F. J. de Heer, M. J. van der Wiel, and J. Kistemaker, "Ionization cross sections for electrons (0.6–20 keV) in noble and diatomic gases," Physica **31**, 94 (1965).
[113]T. D. Märk, "Cross section for single and double ionization of N_2 and O_2 molecules by electron impact from threshold up to 170 eV," J. Chem. Phys. **63**, 3731 (1975).
[114]S. Halas and B. Adamczyk, "Cross sections for the production of N_2^+, N^+ and N_2^{2+} from nitrogen by electrons in the energy range 16–600 eV," Int. J. Mass Spectrom. Ion Phys. **10**, 157–160 (1972).
[115]A. Crowe and J. W. McConkey, "Dissociative ionization by electron impact. IV. Energy and angular distributions of N^{2+} from N_2," J. Phys. B: At., Mol. Opt. Phys. **8**, 1765 (1975).
[116]E. Krishnakumar and S. K. Srivastava, "Cross sections for the production of $N^+{}_2$, N^+ + $N^{2+}{}_2$ and N^{2+} by electron impact on N_2," J. Phys. B: At., Mol. Opt. Phys. **23**(11), 1893 (1990).
[117]J. N. Bull, J. W. L. Lee, and C. Vallance, "Electron ionization dynamics of N_2 and O_2 molecules: Velocity-map imaging," Phys. Rev. A **91**, 022704 (2015).
[118]Z. Shen, E. Wang, M. Gong, X. Shan, and X. Chen, "Electron-impact ionization cross sections for nitrogen molecule from 250 to 8000 eV," J. Electron Spectrosc. Relat. Phenom. **225**, 42–48 (2018).
[119]B. Lindsay and M. Mangan, "5.1 ionization: Datasheet from Landolt-Börnstein—Group I elementary particles, nuclei and atoms," in *Interactions of Photons and Electrons with Molecules*, *Springer Materials Vol. 17C* (Springer-Verlag, Berlin, Heidelberg, 2003).
[120]R. F. Stebbings and B. G. Lindsay, "Comment on the accuracy of absolute electron-impact ionization cross sections for molecules," J. Chem. Phys. **114**, 4741–4743 (2001).
[121]R. R. Goruganthu, W. G. Wilson, and R. A. Bonham, "Secondary-electron-production cross sections for electron-impact ionization of molecular nitrogen," Phys. Rev. A **35**, 540 (1987).
[122]J. E. Hudson, M. L. Hamilton, C. Vallance, and P. W. Harland, "Absolute electron impact ionization cross-sections for the C_1 to C_4 alcohols," Phys. Chem. Chem. Phys. **5**, 3162–3168 (2003).
[123]W. Hwang, Y.-K. Kim, and M. E. Rudd, "New model for electron-impact ionization cross sections of molecules," J. Chem. Phys. **104**, 2956–2966 (1996).
[124]R. S. Freund, R. C. Wetzel, and R. J. Shul, "Measurements of electron-impact-ionization cross sections of N_2, CO, CO_2, CS, S_2, CS_2, and metastable N_2," Phys. Rev. A **41**, 5861–5868 (1990).
[125]J. P. Doering and L. Goembel, "Direct experimental measurement of electron impact ionization-excitation branching ratios: 1. Results for N_2 at 100 eV," J. Geophys. Res.: Space Phys. **96**, 16025–16030, https://doi.org/10.1029/91ja01463 (1991).
[126]J. P. Doering and J. Yang, "Direct experimental measurement of electron impact ionization-excitation branching ratios: 3. Branching ratios and cross sections for the N_2^+ $X\,^2\Sigma_g^+$, $A\,^2\Pi_u$, and $B\,^2\Sigma_u^+$ states at 100 eV," J. Geophys. Res.: Space Phys. **102**, 9683–9689, https://doi.org/10.1029/97ja00308 (1997).
[127]L. Goembel, J. Yang, and J. P. Doering, "Direct experimental measurement of electron impact ionization-excitation branching ratios: 2. Angular distribution of secondary electrons from N_2 at 100 eV," J. Geophys. Res.: Space Phys. **99**, 17477–17481, https://doi.org/10.1029/94ja01142 (1994).
[128]T. G. Finn and J. P. Doering, "Elastic scattering of 13 to 100 eV electrons from N_2," J. Chem. Phys. **63**, 4399 (1975).
[129]N. Abramzon, R. B. Siegel, and K. Becker, "Absolute cross section for the formation of N_2^+ ($X\,^2\Sigma_g^+$) ions produced by electron impact on N_2," J. Phys. B: At., Mol. Opt. Phys. **32**, L247 (1999).
[130]N. Abramzon, R. B. Siegel, and K. Becker, "Cross section for the production of N_2^+ ($X\,^2\Sigma_g^+$) ions by electron impact on N_2," Int. J. Mass Spectrom. **188**, 147–153 (1999).
[131]N. Ferreira, L. Sigaud, V. L. B. de Jesus, A. B. Rocha, L. H. Coutinho, and E. C. Montenegro, "Fragmentation of $^{14,15}N_2$ by electron impact investigated using a time-delayed spectroscopic technique," Phys. Rev. A **86**, 012702 (2012).
[132]L. Sigaud and E. C. Montenegro, "Highly selective mechanisms for the production of N_2 and O_2 dications by electron impact," Phys. Rev. A **98**, 052701 (2018).
[133]J. N. Bull, J. W. L. Lee, and C. Vallance, "Quantification of ions with identical mass-to-charge (m/z) ratios by velocity-map imaging mass spectrometry," Phys. Chem. Chem. Phys. **15**, 13796–13800 (2013).
[134]Y. Zhang, X. Wang, L. F. Zhu, D. Lu, R. Hutton, Y. Zou, and B. Wei, "Dissociative ionization of N_2 by fast electron impact: Roles of molecular orbitals," J. Phys. B: At., Mol. Opt. Phys. **50**, 205202 (2017).
[135]T. Trickl, E. F. Cromwell, Y. T. Lee, and A. H. Kung, "State-selective ionization of nitrogen in the $X\,^2\Sigma^+{}_g$ v_+= 0 and v_+ =1 states by two-color (1+ 1) photon excitation near threshold," J. Chem. Phys. **91**, 6006–6012 (1989).
[136]W. J. Marinelli, W. J. Kessler, B. D. Green, and W. A. M. Blumberg, "Quenching of $N_2(a\,^1\Pi_g, v' = 0)$ by N_2, O_2, CO, CO_2, CH_4, H_2, and Ar," J. Chem. Phys. **90**, 2167–2173 (1989).
[137]W. J. Marinelli, W. J. Kessler, B. D. Green, and W. A. M. Blumberg, "The radiative lifetime of $N_2(a\,^1\Pi_g, v = 0–2)$," J. Chem. Phys. **91**, 701–707 (1989).
[138]A. Dora and J. Tennyson, "Electron collisions with CO molecule: Potential energy curves of higher lying CO^- resonant states," J. Phys. B: At., Mol. Opt. Phys. **53**, 195202 (2020).
[139]F. Paniccia, C. Gorse, M. Cacciatore, and M. Capitelli, "Nonequilibrium ionization of nitrogen: The role of stepwise ionization from metastable states in the presence of superelastic electronic collisions," J. Appl. Phys. **61**, 3123–3126 (1987).
[140]D. Gupta, H. Choi, M.-Y. Song, G. P. Karwasz, and J.-S. Yoon, "Electron impact ionization cross section studies of C_2F_x(x = 1–6) and C_3F_x(x = 1–8) fluorocarbon species," Eur. Phys. J. D **71**, 88 (2017).

[141]A. Laricchiuta, R. Celiberto, and G. Colonna, "Electron impact ionization of metastable states of diatomic molecules," Atoms **10**, 2 (2022).
[142]P. B. Armentrout, S. M. Tarr, A. Dori, and R. S. Freund, "Electron impact ionization cross section of metastable $N_2(A\Sigma_u^+)$," J. Chem. Phys. **75**, 2786–2794 (1981).
[143]M.-Y. Lin and R. Ilie, "A review of observations of molecular ions in the Earth's magnetosphere-ionosphere system," Front. Astron. Space Sci. **8**, 745357 (2022).
[144]L. Campbell, D. C. Cartwright, M. J. Brunger, and P. J. O. Teubner, "Role of electronic excited N_2 in vibrational excitation of the N_2 ground state at high latitudes," J. Geophys. Res.: Space Phys. **111**, A09317, https://doi.org/10.1029/2005ja011292 (2006).
[145]C. H. Sheehan and J.-P. St.-Maurice, "Dissociative recombination of N_2^+, O_2^+, and NO^+: Rate coefficients for ground state and vibrationally excited ions," J. Geophys. Res.: Space Phys. **109**, A03302, https://doi.org/10.1029/2003ja010132 (2004).
[146]D. A. Little, K. Chakrabarti, J. Z. Mezei, I. F. Schneider, and J. Tennyson, "Dissociative recombination of N_2^+: An *ab initio* study," Phys. Rev. A **90**, 052705 (2014).
[147]J. R. Peterson, A. Le Padellec, H. Danared, G. H. Dunn, M. Larsson, A. Larson, R. Peverall, C. Strömholm, S. Rosén, M. af Ugglas, and W. J. van der Zande, "Dissociative recombination and excitation of N_2^+: Cross sections and product branching ratios," J. Chem. Phys. **108**, 1978–1988 (1998).
[148]C. Noren, F. B. Yousif, and J. B. A. Mitchell, "Dissociative recombination and excitation of N_2^+," J. Chem. Soc., Faraday Trans. 2 **85**, 1697–1703 (1989).
[149]P. M. Mul and J. W. McGowan, "Merged electron-ion beam experiments. III. Temperature dependence of dissociative recombination for atmospheric ions NO^+, O_2^+ and N_2^+," J. Phys. B: At., Mol. Opt. Phys. **12**, 1591 (1979).
[150]S. L. Guberman, "The vibrational dependence of dissociative recombination: Cross sections for N_2^+," J. Chem. Phys. **139**, 124318 (2013).
[151]A. Abdoulanziz, C. Argentin, V. Laporta, K. Chakrabarti, A. Bultel, J. Tennyson, I. F. Schneider, and J. Z. Mezei, "Low-energy electron impact dissociative recombination and vibrational transitions of N_2^+," J. Appl. Phys. **129**, 053303 (2021).
[152]S. L. Guberman, "The vibrational dependence of dissociative recombination: Rate constants for N_2^+," J. Chem. Phys. **141**, 204307 (2014).
[153]F. J. Mehr and M. A. Biondi, "Electron temperature dependence of recombination of O_2^+ and N_2^+ ions with electrons," Phys. Rev. **181**, 264 (1969).
[154]M. Fifirig, "Dissociation of $^{14}N_2^+$ ions induced by slow electrons," Mol. Phys. **112**, 1910–1917 (2014).
[155]E. M. Bahati, J. J. Jureta, D. S. Belic, H. Cherkani-Hassani, M. O. Abdellahi, and P. Defrance, "Electron impact dissociation and ionization of N_2^+," J. Phys. B: At., Mol. Opt. Phys. **34**, 2963–2973 (2001).
[156]Y. K. Kim, K. K. Irikura, and M. A. Ali, "Electron-impact total ionization cross sections of molecular ions," J. Res. Natl. Inst. Stand. Technol. **105**, 285 (2000).
[157]M.-Y. Song, J.-S. Yoon, H. Cho, G. P. Karwasz, V. Kokoouline, Y. Nakamura, and J. Tennyson, "'Recommended' cross sections for electron collisions with molecules," Eur. Phys. J. D **74**, 60 (2020).